Articles

Synthesis and Biological Evaluation of Substituted [^{18}F]Imidazo[1,2-*a*]pyridines and [^{18}F]Pyrazolo[1,5-*a*]pyrimidines for the Study of the Peripheral Benzodiazepine Receptor Using Positron Emission Tomography

Christopher J. R. Fookes, Tien Q. Pham, Filomena Mattner, Ivan Greguric,* Christian Loc'h, Xiang Liu, Paula Berghofer, Rachael Shepherd, Marie-Claude Gregoire, and Andrew Katsifis

Radiopharmaceuticals Research Institute, Australian Nuclear Science and Technology Organisation, PMB 1 Menai NSW 2234, Sydney, Australia

Received November 19, 2007

The fluoroethoxy and fluoropropoxy substituted 2-(6-chloro-2-phenyl)imidazo[1,2-*a*]pyridin-3-yl)-*N*,*N*-diethylacetamides **8** (PBR102) and **12** (PBR111) and 2-phenyl-5,7-dimethylpyrazolo[1,5-*a*]pyrimidin-3-yl)-*N*,*N*-diethylacetamides **15** (PBR099) and **18** (PBR146) were synthesized and found to have high in vitro affinity and selectivity for the peripheral benzodiazepine receptors (PBRs) when compared with the central benzodiazepine receptors (CBRs). The corresponding radiolabeled compounds [^{18}F]**8** [^{18}F]**12**, [^{18}F]**15**, and [^{18}F]**18** were prepared from their *p*-toluenesulfonyl precursors in 50−85% radiochemical yield. In biodistribution studies in rats, the distribution of radioactivity of the [^{18}F]PBR compounds paralleled the known localization of PBRs. In the olfactory bulbs, where the uptake of radioactivity was higher than in the rest of the brain, PK11195 and Ro 5-4864 were able to significantly inhibit [^{18}F]**12**, while little or no pharmacological action of these established PBR drug were observed on the uptake of [^{18}F]**8**, [^{18}F]**15**, and [^{18}F]**18** compared to control animals. Hence, [^{18}F]**12** appeared to be the best candidate for evaluation as an imaging agent for PBR expression in neurodegenerative disorders.

Introduction

The peripheral benzodiazepine receptor (PBR[a]) is a transmembrane multimeric protein complex primarily located in the outer mitochondrial membrane of cells. It is composed of an 18 kDa isoquinoline carboxamide-binding protein, a 32 kDa voltage dependent anion channel (VDAC), and a 30 kDa adenine nucleotide translocase (ANT).[1] The PBR is predominantly expressed in peripheral organs such as the kidney, heart, and the steroid hormone producing cells of the adrenal cortex, testis, and ovaries.[2] In the CNS, the PBR is distinct from the central benzodiazepine receptor (CBR). In rodents, PBR is found in the ependymal lining of the ventricles, choroid plexus, and the olfactory bulb,[3] where it has been shown to modulate neuronal activity through the production of neurosteroids.[4]

In humans, PBR density is considerably overexpressed in neuroinflammation and neurodegeneration, suggesting that the PBR could be a clinically useful marker for the detection of such disorders. Consequently, radioligands based on the 1,4-benzodiazepine 7-chloro-1,3-dihydro-1-methyl-5(4′-chlorophenyl)-2*H*-1,4-benzodiazepine-2-one (Ro 5-4864)[2,5] and the isoquinoline carboxamide 2-chlorophenyl-*N*-methylpropyl)-3-isoquinolinecarboxamide (PK11195)[3,6] (Figure 1), which can target the PBR, have been shown to measure changes in PBR receptor density in a number of pathological conditions such as neurodegeneration,[7] inflammation,[8] Alzheimer's,[9,10] Parkinson's[11,12] and Huntington's diseases,[13] and multiple sclerosis.[8,14] In neoplastic tissue enhanced PBR, expression has been observed in gliomas,[15,16] breast,[17] colon,[18] ovarian carcinomas,[19] and prostatic adenocarcinomas.[20]

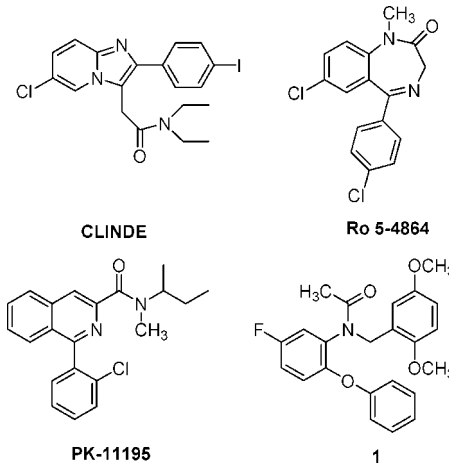

Figure 1. Structures of some established PBR ligands.

Accordingly, analogues of PK11195 and Ro 5-4864 radiolabeled with carbon-11 were able to image several pathological conditions associated with altered PBR expression using the noninvasive imaging modality positron emission tomography (PET),[21] while replacement of the chlorine in PK11195 by

* To whom correspondence should be addressed. Phone: +61 2 9717 3759. Fax: +61 2 9717 9262. E-mail: ivg@ansto.gov.au.

[a] Abbreviations: CNS, central nervous system; DMF, dimethylformamide; EDCI, 1-ethyl-3-(3-dimethylaminopropyl)-carbodiimide; DEA, diethylamine; DIPEA, *N*,*N*′-diisopropylethylamine; HOBT, *N*-hydroxybenzotriazole; $K_{2.2.2}$, 4,7,13,21,24-hexaoxa-1,10-diazabicyco[8.8.8]hexacosane; NMM, *N*-methylmorpholine; RP-HPLC, reverse phase high pressure liquid chromatography; PBR, peripheral benzodiazepine receptor; PET, positron emission tomography; RT, room temperature; PBSF, perfluoro-1-butanesulfonyl fluoride; SAR, structure−activity relationship; TEA.3HF, triethylamine trihydrofluoride; TMHD,*N*,*N*,*N*′,*N*′-tetramethylhexane-1,6-diamine.

10.1021/jm7014556 CCC: $40.75
Published on Web 06/17/2008

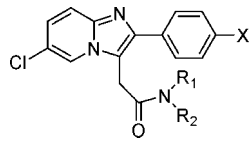

Figure 2. General structure of imidazo[1,2-*a*]pyridines.

iodine-123 enabled imaging with single photon emission computer tomography (SPECT).[22,23] More recently, new ligands, including the imidazo[1,2-b]pyridines,[24,25] [123I]CLINDE,[26] (Figure 1) [11C]CLINME,[27] [123I]CLINME,[28] and the structurally related imidazopyridazines[29] the 2-phenylpyrazolo[1,5-*a*]pyrimidineacetamides [11C]DPA-713,[30] [123I] *N*,*N*-dialkyl-2-phenylindol-3-yl-glyoxylamides,[31] *N*-benzyl-*N*-(2-phenoxyaryl)-acetamide derivatives **1** ([11C]DAA1106)[32,33] (Figure 1), and their structural analogues [11C]pyridinylacetamides,[34] have been developed as potential probes for imaging PBR receptors in vivo using PET or SPECT.

The increasing availability of PET, and the short half-life of carbon-11 has prompted the development of novel [18F] ligands, including the *N*-benzyl-*N*-(2-phenoxyaryl)acetamides[21,35,36] and 2-(2-(4-tert-butylphenyl)-6-fluoroimidazo[1,2-b]pyridazin-3-yl)-*N*,*N*-diethylacetamide (PBR132),[37] with promising preclinical data. Similarly, halogenated 2-phenylimidazopyridines, imidazopyridazines, and pyrazolopyrimidine-3-acetamides have been prepared with high affinity and selectivity for the PBR receptor.[24,29] One aspect of the extensive structure affinity studies carried out in our laboratory[24,29] and elsewhere[38] has revealed that 6-chloro-2-phenylimidazo[1,2-*a*]pyridine-3-yl acetamides (Figure 2), where R_1 and R_2 are small alkyl groups, have high affinity for the PBR when the para-substituent X on the 2-phenyl ring is moderately large. Consequently, a large number of ligands based on this structure have been prepared bearing the SPECT isotope I-123. For example, CLINDM (R_1 and R_2 = Me, X = I) is a potent PBR ligand, while the incorporation of fluorine directly on the 2′-phenyl ring has resulted in a marked increase in CBR affinity and concomitant loss in PBR affinity and selectivity.[24]

However, the observation that a methoxy group in the 4′-position is well tolerated and the associated difficulties in introducing fluorine directly on to these aromatic heterocycles suggested that a short side-chain incorporating a fluorine atom, as in the fluoroethoxy or fluoropropoxy derivatives, could provide compounds of suitable PBR affinity and selectivity as well as providing a convenient route to the efficient incorporation of fluorine-18. Similarly, the methoxy group of the high affinity and selective pyrazolo[1,5-*a*]pyrimidine **13**[39] could also be replaced by the larger fluoroethoxy and fluoropropoxy substituents, providing potentially higher affinity PBR compounds for applications in PET imaging.

In this work, the fluoroethoxy and fluoropropoxy substituted 2-(6-chloro-2-phenyl)imidazo[1,2-*a*]pyridin-3-yl)-*N*,*N*-diethylacetamides **8** (PBR102)[29] and **12** (PBR111)[29] [Scheme 1] and 2-phenyl-5,7-dimethylpyrazolo[1,5-*a*]pyrimidin-3-yl)-*N*,*N*-diethylacetamides **15** (PBR099)[29] and **18** (PBR146)[29] [Scheme 2] were synthesized and their affinities for both the PBR and the CBR evaluated. The corresponding [18F]fluoroalkoxy derivatives were subsequently prepared via nucleophilic radiofluorination from their *p*-toluenesulfonyl precursors and their radiopharmacological properties assessed.

Results and Discussion

Chemistry. The synthesis of the four target molecules **8**, **12**, **15**, and **18** and their corresponding *p*-toluenesulfonyl precursors required for fluorine-18 labeling are shown in Schemes 1 and 2.

The synthesis of the imidazo[1,2-*a*]pyridine scaffold **2** was achieved by condensing 2-amino-5-chloropyridine with 2′-bromo-4-methoxyacetophenone. The acetic acid side-chain was introduced at position −3 by a four-step procedure starting with Mannich condensation with formaldehyde and dimethylamine to give **3**, followed by quaternization with methyl iodide. The resulting salt **4** underwent reaction with potassium cyanide in refluxing ethanol/water to give the amide **5** resulting from hydrolysis of the intermediate nitrile under the strongly alkaline reaction conditions. This was demethylated and further hydrolyzed to the phenolic acid **6** using hydrobromic acid in acetic acid. During the formation of the key diethylamide intermediate **7** (using EDCI, HOBT, and DIPEA), there was significant reaction between the phenol and carboxyl groups, producing 30−50% of dimeric and trimeric species. This unwanted reaction was reversed by treating the crude product with diethylamine in DMF. Alkylation of the phenol group of **7** with 1-bromo-2-fluoroethane in DMF, using potassium carbonate and potassium iodide in the presence of the phase transfer catalyst tetrabutylammonium iodide, produced **8**. Similarly, 2-bromoethyl acetate gave the acetoxyethyl derivative **9a**, however, the product was accompanied by considerable quantities of the corresponding alcohol **10a**. Subsequent treatment with cesium carbonate in aqueous methanol[40] cleanly converted the acetate **9a** into the alcohol **10a**, which was tosylated using *N*,*N*,*N*′,*N*′-tetramethylhexane-1,6-diamine (THMD) as a base to give **11a**. The same 2-step procedure was followed to prepare the homologous alcohol **10b**. The product was converted into the corresponding fluoride **12** by treatment with perfluorobutanesulfonyl fluoride and triethylamine trihydrofluoride in the presence of DIPEA.[41] Reaction of **10b** with *p*-toluenesulfonyl chloride and THMD gave the radiolabeling precursor **11b**.

The pyrazolo[1,5-*a*]pyrimidine PBR ligands **15** and **18** were synthesized from the known compound **13**.[14] Boron trichloride-catalyzed demethylation by tetrabutylammonium iodide[42] gave the phenol **14**, which was alkylated with 1-bromo-2-fluoroethane to produce **15**. Alkylation of **14** with either 2-bromoethyl acetate or 3-bromopropyl acetate, followed by cesium carbonate hydrolysis (without purification of the intermediate acetates), yielded the alcohols **16a** and **16b**, respectively. Compound **17b** was then converted into **18** by the same method used for **12**. Finally, tosylation of **16a** and **16b** gave the radiolabeling precursors **17a** and **17b**.

Radiochemistry. Radiofluorination was achieved via nucleophilic substitution of the *p*-toluenesulfonyl precursor (**11a**, **11b**, **17a**, or **17b**) by [18F]fluoride in the presence of equimolar ratios of $K_{2.2.2}$ and K_2CO_3 as shown in Scheme 3. Azeotropic drying in acetonitrile was performed twice, before the dried K[18F]F−$K_{2.2.2}$ complex was treated with the *p*-toluenesulfonyl precursor in anhydrous acetonitrile. The reactions were heated with stirring at 100 °C for 5 min (Table 1) to form the radiofluorinated products and quenched with mobile phase before injection onto a preparative HPLC column for purification. The overall radiosynthesis, including [18F]fluorination, HPLC purification, evaporation, and radiotracer formulation was completed in a time range of 60−90 min with a radiochemical

Scheme 1. Synthesis of **8** and **12** and the *p*-Toluenesulfonyl Radiolabelling Precursors **11a** and **11b**[a]

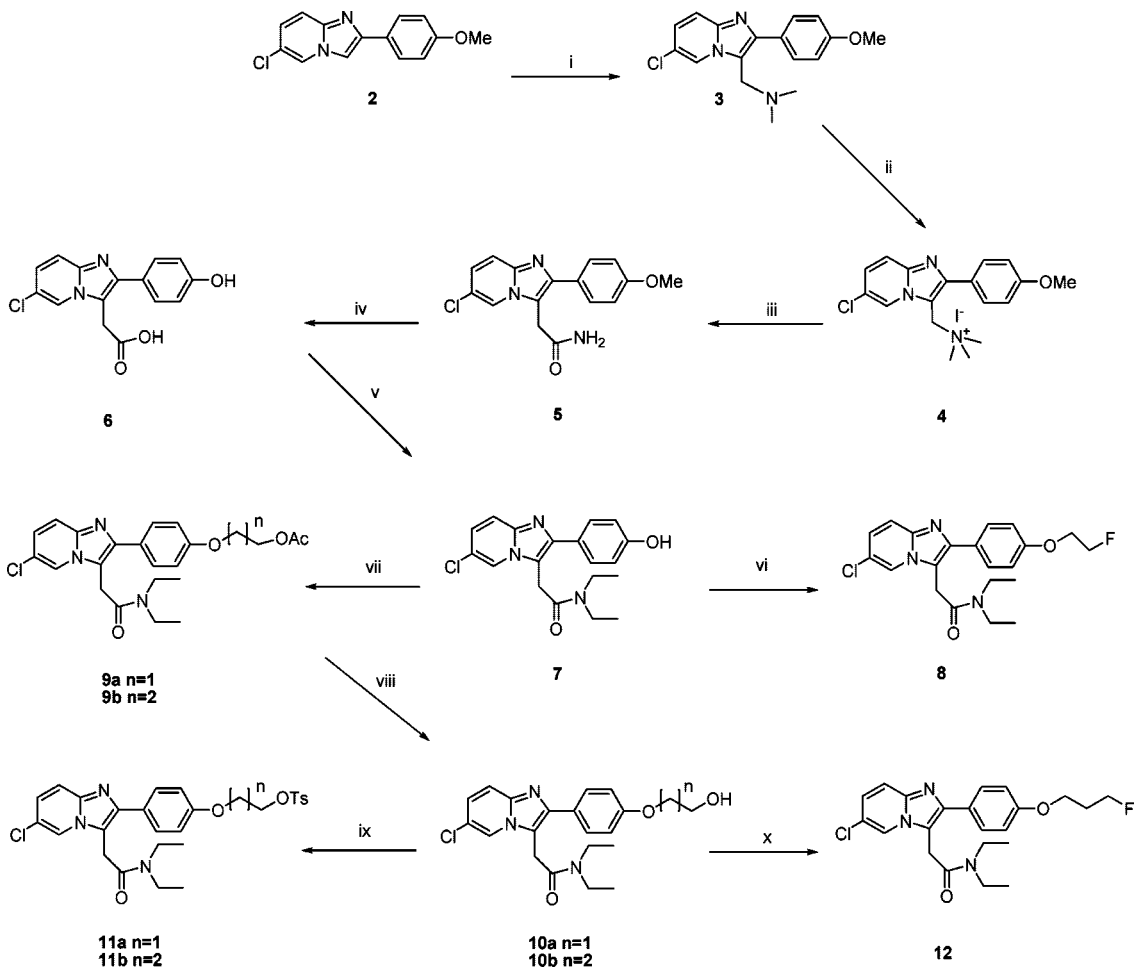

[a] (i) $(CH_3)_2NH$ (aq), CH_2O, CH_3COOH, 60 °C, 20 h; (ii) CH_3I, benzene, RT, 18 h; (iii) KCN, EtOH/H_2O 1:1, reflux, 24 h; (iv) HBr, CH_3COOH, reflux, 48 h; (v) EDCI, HOBT, DIPEA, DMF, DEA, RT, 4 days; (vi) K_2CO_3, KI, Bu_4NI, 1-bromo-2-fluoroethane, 48 h; (vii) K_2CO_3, KI, 2-bromoethyl acetate (**9a**) or 3-bromopropyl acetate (**9b**) Bu_4NI at RT for 48 h; (viii) Cs_2CO_3, MeOH, H_2O, RT, 48 h; (ix) TsCl, TMHD, CH_3CN, RT, 15 h; (x) DIPEA, PBSF, TEA.3HF CH_3CN, 40 °C, 30 min then RT, 12 h.

Scheme 2. Synthesis of **15** and **18** and the Corresponding *p*-Toluenesulfonyl Precursors **17a** and **17b**[a]

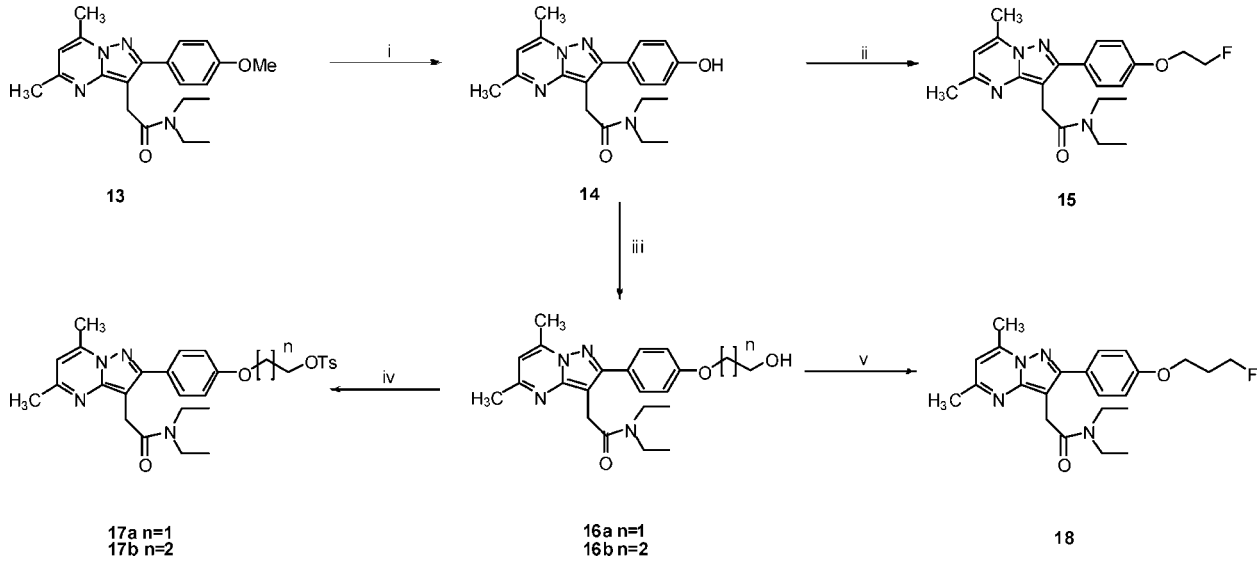

[a] (i) Bu_4NI, BCl_3, DCM, −70 °C, 5 min, then 4 °C for 2.5 h; (ii) K_2CO_3, KI, Bu_4NI, 1-bromo-2-fluoroethane, DMF, RT, 48 h; (iii) K_2CO_3, KI, 2-bromoethyl acetate (**16a**) or 3-bromopropyl acetate (**16b**), Bu_4NI, DMF, RT, 48 h; (vi) Cs_2CO_3, MeOH, H_2O, RT, 48 h; (v) TsCl, TMHD, CH_3CN at RT; (iv) DIPEA, PBST, TEA.3HF, CH_3CN, 40 °C, 30 min, then RT 12 h.

purity greater than 95%. The identity of the [^{18}F]compounds ([^{18}F]**8**, [^{18}F]**12**, [^{18}F]**15**, and [^{18}F]**18**) was confirmed by coinjection of their corresponding unlabeled compound using analytical HPLC conditions (Table 1).

Scheme 3. Radiolabelling of [18F]Imidazo[1,2-*a*]pyridines and [18F]Pyrazolo[1,5-*a*]pyrimidines

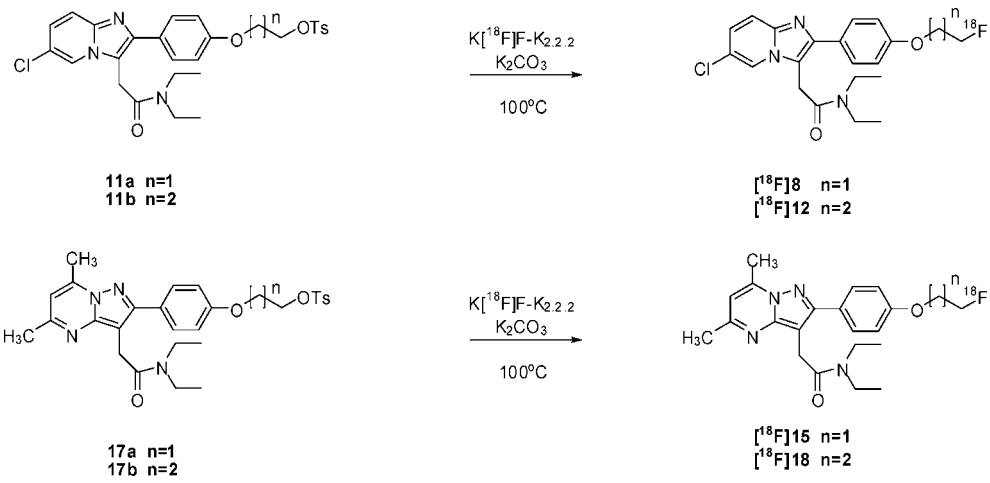

Table 1. Radiolabelling Data for the [18F]PBR Radiotracers

[18F] compound	precursor[a]	purification solvent[b]	retention time (min)	RCY%[e]	QC solvent
[18F]**15**	**17a**	40/60[a]	13	55−85	30/70[f]
[18F]**8**	**11a**	45/55[d]	13	55−75	45/55[g]
[18F]**18**	**17b**	40/60[c]	12	50−67	50/50[g]
[18F]**12**	**11b**	45/55[d]	13	56−75	30/70[f]

[a] Precursor mass of 2 mg, reacting at 100 °C, 5 min. [b] Acetonitrile/H_2O + 0.1%TFA. [c] Waters X-Bridge C18 (10 μm, 30 mm × 100 mm), 15 mL/min. [d] Grace Alltima C18 (10 μm; 22 mm × 250 mm), 10 mL/min. [e] Isolated yield (decay corrected), specific activity 110−150 GBq/μmol. [f] Phenomenex Luna C18(2) (5 μm; 4.6 mm × 150 mm) 1 mL/min, acetonitrile/H_2O 0.1%TFA. [g] Phenomenex Gemini C18 (5 μm; 4.6 mm × 150 mm), 1 mL/min acetonitrile/0.1 M ammonium acetate.

Table 2. Inhibition Constant (K_i) and log $P_{7.5}$ of Compounds Studied

	K_i[a] PBR ([3H]PK11195)[b]	K_i[a] PBR ([3H]Ro 5-4864)[b]	K_i[a] CBR ([3H]flumazenil)[c]	log $P_{7.5}$
15	5.6 ± 0.9	5.7 ± 0.1	>5000	2.5 ± 0.1
8	5.8 ± 0.4	3.3 ± 0.4	790 ± 90	2.7 ± 0.1
18	4.1 ± 0.4	5.8 ± 0.5	>5000	3.2 ± 0.1
12	3.7 ± 0.4	4.2 ± 0.4	800 ± 120	3.2 ± 0.1

[a] K_i values, expressed in nM, were calculated from the experimental IC_{50} values using the Chen−Prussof equation. [b] [3H]PK11195 and [3H]Ro 5-4864 binding on rat kidney membranes. [c] [3H]Flumazenil binding on brain cortex membranes.

Ligand Binding Assays. The inhibition constant (K_i) for the CBRs as measured with [3H]ethyl 8-fluoro-5,6-dihydro-5-methyl-6-oxo-4*H*-imidazo[1,5-*a*](1,4)benzodiazepine-3-carboxylate ([3H]flumazenil) were 800 nM for the imidazopyridine derivatives **8** and **12** and >5000 nM for the pyrazolopyrimidine compounds **15** and **18** (Table 2). The K_i values for PBR as measured with [3H]PK11195 and [3H]Ro 5-4864 ranged from 3−6 nM. Interestingly, the fluoropropoxy derivatives **12** and **18** were slightly more potent inhibitors of PK11195 binding ($K_i \sim 4$ nM) than the fluoroethoxy derivatives **15** and **8** ($K_i \sim 6$ nM). Similarly, the imidazopyridine analogues, **8** and **12**, were somewhat more potent in inhibiting Ro 5-4864 binding ($K_i \sim 4$ nM) than the pyrazolopyrimidine analogues, **15** and **18** ($K_i \sim 6$ nM). According to these assays, the compounds described here are potent PBR inhibitors with low CBR affinity.

Biodistribution Studies. The time-course distribution of the radiofluorinated tracers in rats is presented in Table 3. In the kidney and in the heart, the radioactivity concentration peaked between 0.25 and 1 h post injection and then decreased. In early time points, the heart radioactivity uptake (8−9%ID/g) after injection of the fluoropropoxy derivatives [18F]**12** and [18F]**18** were 70% higher than the fluoroethoxy compounds [18F]**15** and [18F]**8** (4−5%ID/g). Similarly, after injection of [18F]**12** and [18F]**18**, the kidney radioactivity uptake (5%ID/g) was 45% higher than that of the fluoroethoxy compounds [18F]**15** and [18F]**8** (3.5%ID/g). Radioactivity uptake in the lungs of all radiotracers decreased over time from an initial value 14−20%ID/g at 0.25 h to 3−6%ID/g at 4 h. In the spleen, the radioactivity uptake decreased over time from 5−6% to 2−4%ID/g for all radiotracers except for [18F]**15**, where the uptake remained constant (4.5%ID/g) over the course of 4 h. In the steroidogenic organs, after injection of the [18F]PBR ligands, the radioactivity uptake in adrenals and in testis was 5−8%ID/g and 0.2−0.3%ID/g, respectively, at 0.25 h and increased slowly with time.

The initial blood radioactivity concentration following [18F]**8** and [18F]**15** injection decreased from an initial 0.2% to almost 0.1%ID/g in the first hour but was then followed by a slow increase with time. This small incremental increase could be related to the specific metabolism of the two compounds. The blood radioactivity concentration for the fluoropropoxy derivatives [18F]**12** and [18F]**18** were initially high (0.3−0.4%ID/g at 0.25 h), which also decreased rapidly, falling to 0.1%ID/g at 4 h (Figure 3). In the brain, the radioactive concentration displayed the same kinetics as the blood irrespective of the radiofluorinated tracer studied, so the displayed brain to blood concentration ratios were constant over time, indicating an equilibrium between brain and blood. Although no direct relationship between lipophilicity and brain uptake could be made in this study, all four compounds displayed lipophilicity values (log $P_{7.5}$) ranging from 2.5 to 3.2, which is in the range favored for blood brain barrier permeability (Table 2).

At 0.25 h, the olfactory bulbs showed 50 and 70% higher radioactivity concentration than the brain for the pyrazolopyrimidine derivatives [18F]**18** and [18F]**15**, respectively, while the radioactivity concentration in the olfactory bulbs for the imidazopyridine derivatives [18F]**8** and [18F]**12** were, respectively, 150 and 170% higher than the corresponding concentration in the brain. The activity in the olfactory bulbs remained constant or slowly decreased during the study. The olfactory bulb to blood concentration ratios were constant (∼2) over the duration of the study for [18F]**15** and [18F]**8**, but as a consequence of the decrease in activity in the blood, the ratios increased with time and were 3 and 5 at 4 h for [18F]**18** and [18F]**12**, respectively.

In the femur, the uptake of radioactivity increased over time (Figure 4). This uptake was 0.4%ID/g at 0.25 h and reached

Table 3. Biodistribution of [^{18}F]PBR Compounds in Rats

	time (h)	kidney[a]	heart[a]	lungs[a]	spleen[a]	liver[a]	adrenals[a]	testis[a]
[^{18}F]**15**	0.25	3.8 ± 0.2	5.8 ± 0.4	14.6 ± 1.3	4.6 ± 0.3	0.63 ± 0.06	5.6 ± 0.5	0.18 ± 0.01
	0.5	3.6 ± 0.5	5.6 ± 0.3	8.8 ± 0.5	4.7 ± 0.6	0.54 ± 0.18	6. Six ± 1.2	0.21 ± 0.01
	1	3.5 ± 0.2	6.4 ± 0.4	5.7 ± 0.6	4.5 ± 0.7	0.40 ± 0.05	7.8 ± 1.7	0.27 ± 0.02
	4	2.4 ± 0.4	4.3 ± 0.9	2.8 ± 0.5	3.9 ± 0.6	0.29 ± 0.04	9.7 ± 1.5	0.35 ± 0.01
[^{18}F]**8**	0.25	3.3 ± 0.37	4.3 ± 0.3	14.3 ± 1.4	4.5 ± 0.5	0.63 ± 0.15	6.7 ± 1.3	0.17 ± 0.01
	0.5	3.2 ± 0.5	4.4 ± 0.3	12.1 ± 2.0	3.9 ± 0.4	0.52 ± 0.14	7.9 ± 1.7	0.23 ± 0.03
	1	2.7 ± 0.2	4.6 ± 0.3	11.6 ± 1.5	3.4 ± 0.2	0.35 ± 0.01	7.3 ± 1.1	0.31 ± 0.03
	4	1.3 ± 0.1	2.8 ± 0.2	8.1 ± 1.1	1.9 ± 0.2	0.29 ± 0.02	7.1 ± 1.0	0.42 ± 0.01
[^{18}F]**18**	0.25	5.5 ± 1.2	9.0 ± 0.7	20 ± 4	5.5 ± 0.9	1.08 ± 0.05	8.0 ± 0.7	0.27 ± 0.02
	0.5	4.9 ± 0.2	9.0 ± 0.5	12.4 ± 1.3	5.5 ± 0.4	0.98 ± 0.21	7.9 ± 1.5	0.28 ± 0.02
	1	4.7 ± 0.2	8.7 ± 1.0	7.1 ± 0.9	5.1 ± 0.4	0.69 ± 0.26	11.0 ± 2.0	0.32 ± 0.03
	4	3.2 ± 0.3	5.8 ± 0.9	3.3 ± 0.2	3.6 ± 0.2	0.38 ± 0.09	12.2 ± 1.6	0.43 ± 0.04
[^{18}F]**12**	0.25	4.3 ± 0.6	7.8 ± 0.5	12.3 ± 0.5	5.5 ± 0.5	1.08 ± 0.09	8.5 ± 1.4	0.33 ± 0.02
	0.5	5.0 ± 0.3	8.3 ± 0.2	7.7 ± 0.5	6.0 ± 0.4	0.79 ± 0.07	11.8 ± 2.5	0.43 ± 0.02
	1	3.7 ± 0.2	6.4 ± 0.2	4.1 ± 0.3	4.5 ± 0.3	0.61 ± 0.11	9.6 ± 0.5	0.41 ± 0.02
	4	1.8 ± 0.3	2.9 ± 0.3	2.2 ± 0.3	2.5 ± 0.4	0.30 ± 0.07	11.4 ± 1.8	0.53 ± 0.01

[a] Results are the mean of %ID/g of tissue ± SD, $n = 4$.

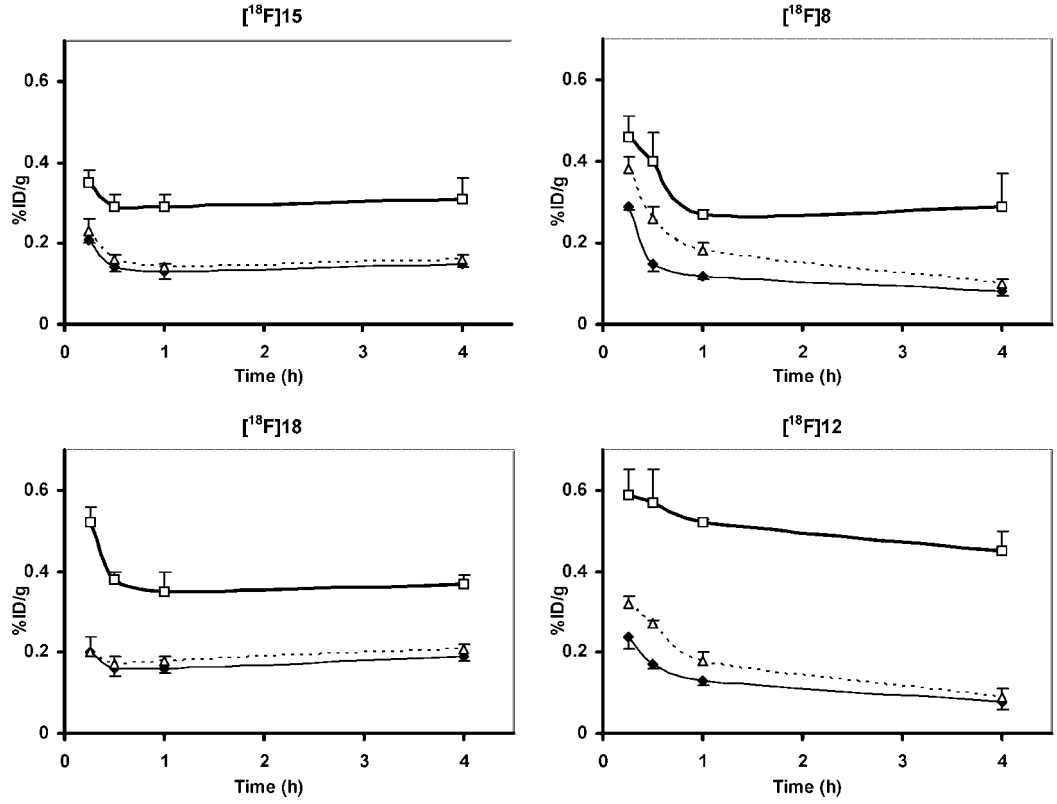

Figure 3. Time course distribution of [^{18}F]**15**, [^{18}F]**8**, [^{18}F]**18**, and [^{18}F]**12** in olfactory bulbs (□), brain (◆), and blood (△). The radioactive concentration is expressed in %ID/g and the error bars represent the standard deviation of the mean value ($n = 4$).

0.7%ID/g at 4 h for both [^{18}F]**15** and [^{18}F]**8**. For [^{18}F]**18** and [^{18}F]**12**, the femur uptake was 0.6 and 2.2%ID/g at 0.25 and 4 h post injection, respectively. The higher radioactive concentration in bone after injection of the fluoropropoxy compounds versus the fluoroethoxy derivatives was investigated. The radioactivity concentration in femur bone marrow, in femur, and in the skull frontal bone (bone with less marrow than femur) were followed after injection of [^{18}F]**12** in rats. In bone marrow, the radioactivity concentration was 2.4 and 1.2 times higher than those of skull at 0.25 and 4 h, respectively. In the skull, the radioactivity concentration was half of that in the femur during the time course of the study. Hence, after injection of [^{18}F]**12**, the bone marrow radioactivity, reflecting PBR expression in the marrow, amounted to 60 and 40% of the total activity of the femur at 0.25 and 4 h, respectively. The majority of the remaining activity is likely to be specific [^{18}F]fluoride adsorption in the bone apatite.

Competition Studies. Drug saturation and competition experiments were carried out to test the ability of central and peripheral drugs to inhibit [^{18}F]PBR radiotracer uptake in peripheral organs and in the brain. The saturating effect of the unlabeled compounds **15**, **8**, **18**, and **12** (1 mg/kg) on the radioactivity uptake of the corresponding [^{18}F]labeled compounds in the heart was observed, with very significant decreases greater than 82% ($p < 0.01$) compared to the heart radioactivity uptake of untreated animals (Figure 5). This saturating effect was also observed in the kidney, with decreases in uptake exceeding 76% ($p < 0.01$), and in the spleen (80%, $p < 0.01$) but not in adrenals.

The administration of the unlabeled fluoroethoxy compounds prior to the radiotracer increased significantly the brain (**15** and **8**) and the olfactory bulb radioactivity uptake (**8**) for the corresponding F-18 compounds that paralleled the increase in blood radioactivity concentration. No effect was observed with

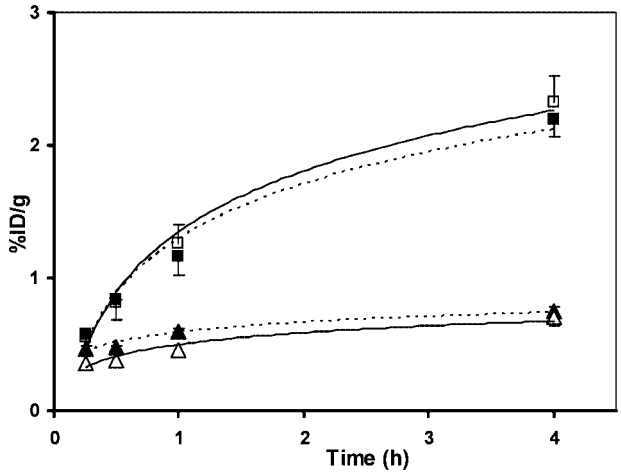

Figure 4. Time course uptake in rat femur of [18F]**15**(△), [18F]**8** (▲), [18F]**18** (■), and [18F]**12** (□). The radioactive concentration is expressed in %ID/g and the error bars represent the standard deviation of the mean value ($n = 4$).

18 and **12** on the brain radioactivity uptake for [18F]**18** and [18F]**12**. In the olfactory bulbs, the administration of the **12** decreased [18F]**12** uptake by 45%, ($p < 0.01$) despite increases in blood radioactive concentration of 33%.

The competitive effect of PK11195 on the radioactivity uptake in the kidney, heart, and the spleen following [18F]PBR injection was higher than the effect of Ro 5-4864, with decreases of 70 to 85% ($p < 0.01$) for PK11195 and decreases of 30 to 70% for Ro 5-4864 observed. In these three organs, the highest inhibition was observed for the radiotracer [18F]**12**.

In the adrenals, pretreatment of the rats with PK11195 or Ro 5-4864 significantly increased the radioactivity concentrations of [18F]**15**, [18F]**8**, and [18F]**18** by 50−100%. These particular effects of the PBR drugs could be explained by an increased concentration of the respective radiotracers [18F]**15**, [18F]**8**, and [18F]**18** made available in the blood after displacement from other tissue or that a component of the radioactivity in the adrenals could be due to nonspecific binding. For [18F]**12**, no significant increase of radioactivity concentration was seen in rats that received PK11195.

The effect of PK11195 and Ro 5-4864 in the brain were similar, as these two PBR drugs were unable to displace the radioactivity (Figure 5). Increases, probably due to the blood were observed for [18F]**15** and [18F]**8**. In the olfactory bulbs, however, PK11195 and Ro 5-4864 were able to inhibit significantly ($p < 0.01$) the uptake of [18F]**12** by 55 and 36%, respectively, while no or minimal pharmacological action of the two PBR drugs were observed on the radioactivity uptake of [18F]**8**, [18F]**15**, and [18F]**18** compared to control animals. When the animals received flumazenil, a CBR drug, the uptake of the radiofluorinated PBR ligands were not significantly different to controls in all the organs and the brain structures studied.

In competition studies, we were unable to significantly inhibit the radioactivity uptake of the fluoroethoxy compounds [18F]**15** and [18F]**8** in the olfactory bulbs, while a very significant inhibition was observed for [18F]**12**. On the other hand, the radioactivity uptake of fluoropropoxy compounds [18F]**18** and [18F]**12** in the bone was higher than that for the fluoroethoxy derivatives. These results may be due to the different in vivo metabolic pathways of the respective radiotracers.

Metabolite Studies. The stability of the [18F]PBR compounds in vivo was studied over 4 h after iv injection. The determination of unchanged tracer was carried out by radio-HPLC. After ultrasonic disruption and protein elimination, at least 85% of the radioactivity in the olfactory bulbs and 75% in the cortex was recovered in the supernatant of 0.25 and 0.5 h samples for HPLC analysis. For later time points, the recovery was still greater than 70% and 60%, respectively, in these tissues. Further extraction of protein precipitate using pure acetonitrile removed almost all radioactivity. Analysis of this extract using radio TLC and solid phase extraction showed it contained only radioactive metabolites.

In plasma, rapid decrease of unchanged radiofluorinated tracers was observed. The amount of parent compounds was approximately 10% for [18F]**18** and [18F]**12** at 0.25 h post injection and less than 1% for [18F]**15** and [18F]**8** at 4 h (Figure 6). In the cortex, 55−80% of the radioactivity represented [18F]PBR compounds at 0.25 h. These values dropped to 10% for [18F]**15** and [18F]**8** and to 30% for [18F]**18** and [18F]**12** at 4 h. In olfactory bulbs, the fraction of unchanged tracer was higher than in the cortical region. For [18F]**15** and [18F]**8**, the percentage of unchanged ligand diminished from 80% at 0.25 h to 40% at 4 h post injection. For [18F]**18** and [18F]**12**, more than 80% of the radioactivity still represented unchanged radiotracer at 4 h pi.

Considering the chemical structures of the studied compounds, it appeared that the amount of unchanged fluoropropoxy derivatives [18F]**18** and [18F]**12** in the brain were much higher than the fluoroethoxy derivatives[18F]**15** and [18F]**8**. Moreover, in the olfactory bulbs, the percentage of unmetabolized fluoropropoxy derivatives were almost constant versus time and higher than 86% for [18F]**12**. By using water as eluent in the first step of HPLC analysis, it was shown that the main radioactive metabolites in plasma, cortex, and olfactory bulbs were highly polar products as they eluted with the solvent front. The remaining radioactivity was analyzed using a gradient system in the second HPLC step; no compounds more lipophilic than the parent compound were observed.

The metabolite and bone uptake results are consistent with the expected fate of the [18F]-containing moiety of the four PBR ligands in vivo. Alkyl aryl ethers are known to dealkylate in mammals by a monooxygenase-mediated reaction that occurs by hydroxylation of the carbon α to the oxygen.[43,44] Cleavage of the resulting hemiacetal generates an aliphatic aldehyde, which in the case of the fluoroethoxy compounds [18F]**15** and [18F]**8** would be [18F]fluoroacetaldehyde. In related studies, using the PET imaging agent 18F-FECNT, [18F]fluoroacetaldehyde (or its oxidation product [18F]fluoroacetic acid) was proposed to be the radiometabolite that accumulates in rat, human, and nonhuman primate brain and was implicated in confounding radioligand measurements.[45] These metabolites would not compete with PK11195 or Ro 5-4864 in the present competition study. In contrast, 3-[18F]fluoropropionic acid, an expected metabolite from [18F]**18** and [18F]**12**, is known to be completely catabolized to inorganic fluoride,[46] which is rapidly sequestered by bone. However, the resulting higher bone uptake of activity observed with [18F]**18** and [18F]**12** versus [18F]**15** and [18F]**8** is still acceptable for PET imaging.

Summary

The PBR compounds described here have nanomolar inhibition constants (K_i) for the PBR specific ligands PK11195 and Ro 5-4864 and micromolar K_i values for the CBR ligand flumazenil. The pyrazolopyrimidine derivatives **15** and **18** bearing the fluoroethoxy and fluoropropoxy substituent on the phenyl group displayed similar affinity and selectivity to the

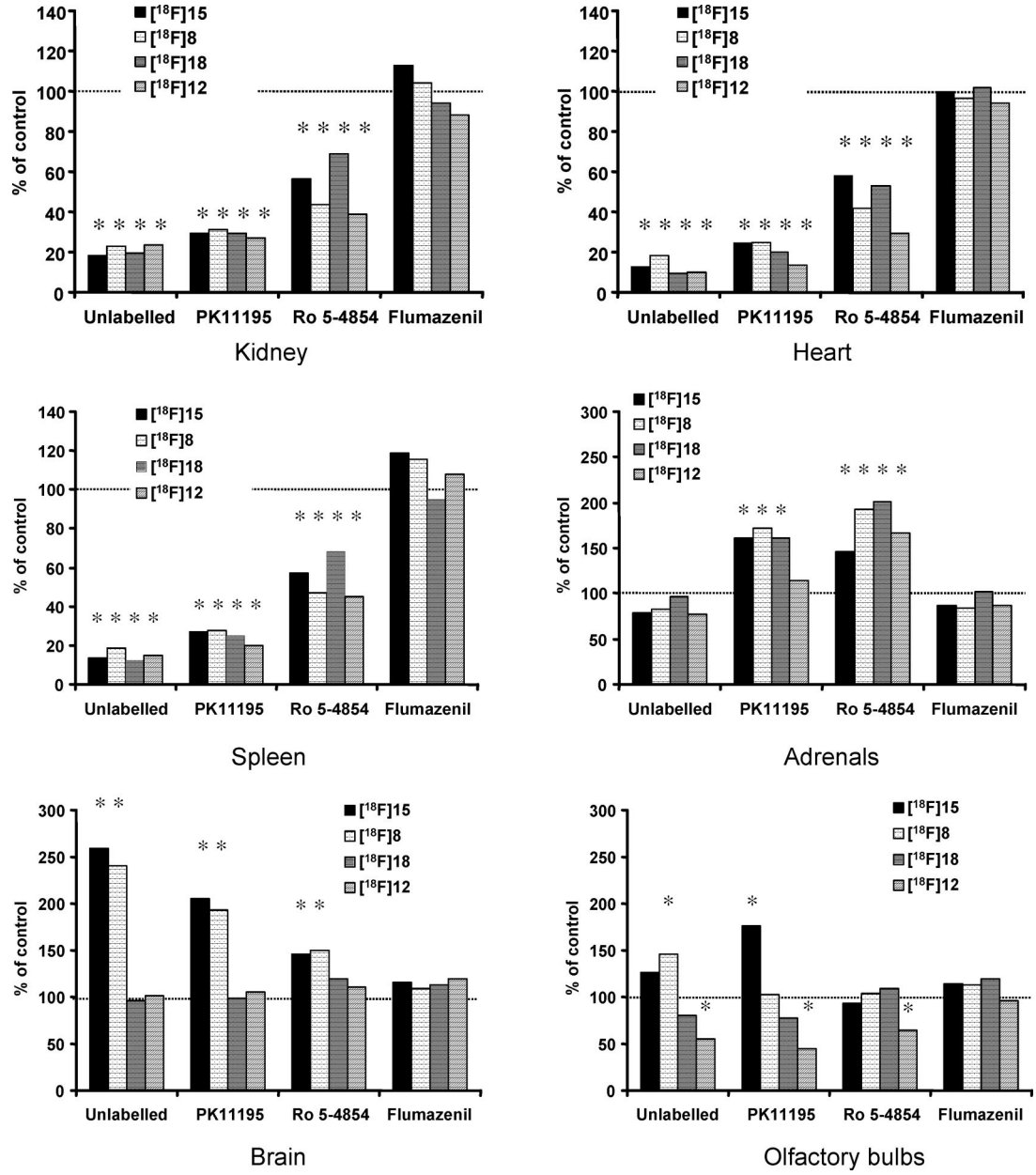

Figure 5. Relative uptake of the [^{18}F]PBR compounds in the kidney, heart, spleen, adrenals, brain, and in the olfactory bulbs in animals treated with the corresponding unlabeled PBR ligand, PK11195, Ro 5-4864, and flumazenil in comparison to untreated animals. For an organ, the relative uptake value is the ratio of the mean radioactive concentrations of treated animals divided by the mean radioactive concentrations of control animals and is expressed in %. *At least $p < 0.05$ calculated using ANOVA test.

methoxy compound **13**. The imidazopyridines **8** and **12** presented similar affinity for PBR but were found to be at least 50 times more selective for PBR versus CBR than the parent compound alpidem.[47]

In peripheral organs, the distribution of radioactivity after injection of the [^{18}F]PBR compounds paralleled the localization of PBRs that are reported to be present in high density in endocrine tissues such as adrenal glands and in organs such as kidney and heart.

In the brain, after injection of [^{18}F]PBR compounds, the uptake in the olfactory bulbs was higher than in the other brain structures throughout the experiment. This is likely related to PBRs, as this region is known to have a higher density of peripheral binding sites than other parts of the brain as measured in vitro with the benzodiazepine [^{3}H]Ro 5-4864 and with the imidazopyridine [^{3}H]CB 34,[48] and in ex vivo autoradiography with the *N*-(5-fluoro-2-phenoxyphenyl)-*N*-(2-[^{18}F]fluoromethyl-5-methoxybenzyl- acetamide and *N*-(5-fluoro-2-phenoxyphenyl)-*N*-(2-[^{18}F]fluoroethyl-5-methoxybenzylacetamide. The specific to nonspecific uptake, calculated as the ratio of the radioactive concentration in olfactory bulbs to the brain, was 4 at 1 h post injection for [^{18}F]**12** while the ratios were ~2 for the other radiotracers. The inability to significantly inhibit the uptake of the fluoroethoxy compounds [^{18}F]**15** and [^{18}F]**8** in the olfactory bulbs while a very significant inhibition was observed for [^{18}F]**12** using the PBR drugs PK11195 and Ro 5-4864 demonstrates that the uptake of [^{18}F]**12** is related to a specific binding on the PBRs. This and the observation that the uptake of radioactivity in the bone after injection of the fluoropropoxy compounds [^{18}F]**18** and [^{18}F]**12** was higher than the fluoroethoxy derivatives suggests that it may be due to the different in vivo metabolic pathways of the respective radiotracers.

In conclusion, among the two series of compounds, [^{18}F]**12** appears to be the most promising radiofluorinated ligand as it

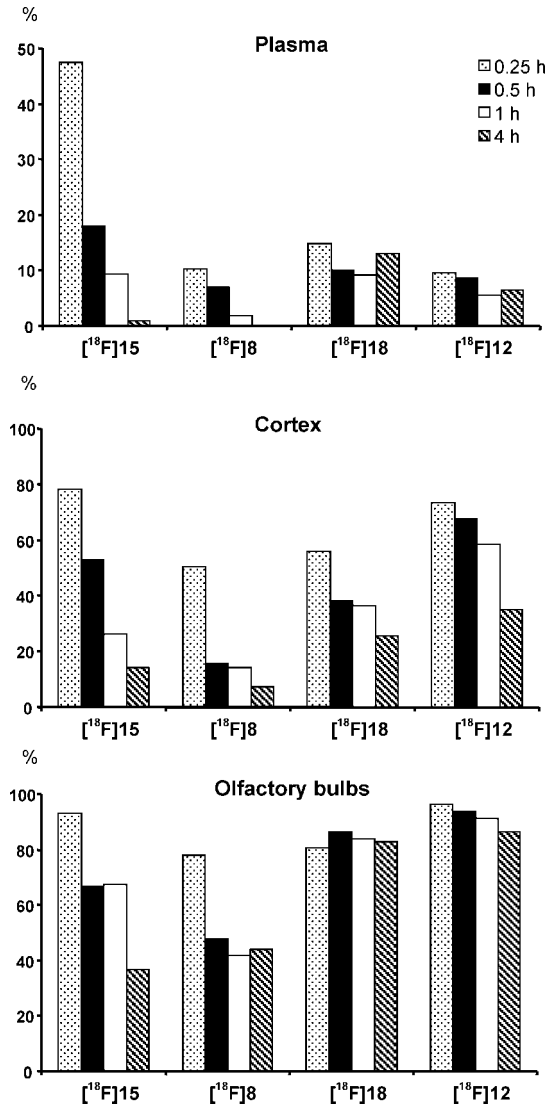

Figure 6. Percentage of unmetabolized [18F]**15,** [18F]**8**, [18F]**18**, and [18F]**12** in plasma, brain cortex, and olfactory bulbs 0.25, 0.5, 1, and 4 h after injection, as measured using radio-HPLC.

possesses the requisite pharmacological profile for brain imaging PBR expression in neurodegenerative disorders.

Experimental Section

General. *N,N*-Diethyl-2-(2-(4-methoxyphenyl)-5,7-dimethylpyrazolo[1,5-*a*]pyrimidin-3-yl)acetamide[49] and 3-bromopropyl acetate[50] were synthesized using literature procedures. 1-Bromo-2-fluoroethane was purchased from Matrix Scientific (USA). Flumazenil, PK11195, and Ro 5-4864 were obtained from Sigma-RBI. [3H]Flumazenil (3.2 MBq/nmol) and [3H]PK11195 (2.8 MBq/nmol) were obtained from Perkin-Elmer. [3H]Ro 5-4864 (3.1 MBq/nmol) was obtained from American Radiolabeled Chemicals. [18F]HF was produced by Cyclotek, Melbourne, Australia, via the $^{18}O(p, n)$ reaction. All other chemicals were purchased from Sigma-Aldrich and used without further purification. Melting points were determined in open capillary tubes using a Gallenkamp melting point apparatus and are uncorrected. NMR spectroscopy was performed on a Bruker Advance DPX 400 operating at 400 MHz for ^{1}H NMR spectra and 100 MHz for ^{13}C NMR spectra. Elemental analyses were determined at the Campbell Microanalytical Laboratory, Department of Chemistry, University of Otago, New Zealand. Low resolution mass spectrometry (LRMS) was performed on a Micromass ZMD quadrupole mass spectrometer, while high resolution mass spectrometry (HRMS) was performed using a Bruker Daltonics BioApex-II 7T FTICR mass spectrometer equipped with an off-axis analytical ESI source. Preparative HPLC was performed on a Waters Empower system, equipped with a 600 gradient pump and a 996 PDA detector, 717 autosampler, and fraction collector III. Purification of the radiotracers was performed on a radio-HPLC system equipped with Waters 486 UV, set at 254 nm, and an Ortec Acemate Scint 925 γ-detector with a sodium iodide crystal. For radiochemical purity and stability measurements, the radiofluorinated tracer was ascertained on an analytical HPLC system equipped with a Varian 9002 pump, linear UV detector set at 254 nm, and an Ortec Acemate Scint 925 γ-detector with a sodium iodide crystal using Laura version 3 software package. The radiochemical and chemical purity and specific activity measurements were confirmed on an analytical HPLC using a C18 analytical column (Table 1). Metabolite studies were performed on a system consisting of a (Waters) 600 gradient pump, a 486 UV detector set at 254 nm, a 717 autosampler and an in line detector for measurement of radioactivity (β-Ram IN/US) operated by Waters Empower software.

6-Chloro-2-(4-methoxyphenyl)imidazo[1,2-*a*]pyridine (2). A mixture of 2-bromo-4′-methoxyacetophenone (25 g, 110 mmol), 2-amino-5-chloropyridine (14.0 g, 109 mmol), and absolute ethanol (220 mL) was stirred at reflux for 2 h. $NaHCO_3$ (5.5 g, 65 mmol) was then added and heating continued for another 6 h. Additional $NaHCO_3$ (3.65 g, 43 mmol) was then added and stirring continued for a further 15 min. The mixture was cooled to 4 °C for 12 h and the solid was filtered, washed with cold ethanol (50 mL), water (100 mL), then ethanol (30 mL). The solid was then boiled with ethanol (100 mL) for 10 min, cooled, and filtered. The solid was washed with ethanol (30 mL) again and dried in vacuo to give a pale-yellow powder (21 g, 83%); mp 220−222 °C. ^{1}H NMR (DMSO-d_6) δ: 3.80 (s, 3H), 7.01 (d, J = 8.8 Hz, 2H), 7.26 (dd, J = 9.6, 2.0 Hz, 1H), 7.59 (d, J = 9.6 Hz, 1H), 7.89 (d, J = 8.8 Hz, 2H), 8.26 (s, 1H), 8.78 (dd, J = 2.0, 0.8 Hz, 1H). ^{13}C NMR (DMSO-d_6) δ: 55.1, 108.7, 114.2, 117.2, 118.7, 124.6, 125.5, 126.0, 127.0, 143.2, 145.5, 159.2. MS ES(+ve) m/z 259 (M + 1).

1-(6-Chloro-2-(4-methoxyphenyl)imidazo[1,2-*a*]pyridin-3-yl)-*N,N*-dimethylmethanamine (3). Compound (**2**) (20.7 g, 80 mmol) in acetic acid (250 mL) was slowly treated with aqueous dimethylamine (40%, 127 mL) followed by aqueous formaldehyde (37%, 51 mL) and the mixture stirred at 55 °C for 20 h. After cooling, the solution was concentrated, and the syrupy residue was dissolved in a mixture of water (100 mL) and chloroform (200 mL). Aqueous NaOH (10%) was added; until the pH was 12, the chloroform layer separated and the aqueous phase was further extracted with chloroform (2 × 50 mL). The combined chloroform solutions were then extracted with 2N HCl (3 × 100 mL) and the extract partially neutralized with NaOH (15 g) to pH 3. After standing at RT for 12 h, the precipitate of hydroxymethyl byproduct (2.0 g) was filtered off. The filtrate was then basified to pH 12 with NaOH to afford the product as a thick oil, which slowly solidified. The solid was recrystallized from ethanol/water (18.9 g, 75%); mp 106−107 °C. ^{1}H NMR (DMSO-d_6) δ: 2.16 (br s, 6H), 3.33 (s, 2H), 3.81 (s, 3H), 3.90 (s, 2H), 7.03 (d, J = 8.8 Hz, 2H), 7.31 (dd, J = 9.6, 1.8 Hz, 1H), 7.62 (d, J = 9.6 Hz, 1H), 7.79 (d, J = 8.8 Hz, 2H), 8.63 (d, J = 1.8 Hz, 1H). ^{13}C NMR (DMSO-d_6) δ: 44.4, 51.3, 55.0, 113.8, 117.1, 117.7, 118.4, 123.4, 125.1, 126.4, 129.4, 142.2, 144.4, 158.8. MS ES(+ve) m/z 316 (M + 1). Anal. ($C_{17}H_{18}ClN_3O$) C, H, N.

1-(6-Chloro-2-(4-methoxyphenyl)imidazo[1,2-*a*]pyridin-3-yl)-*N,N,N*-trimethylmethanammonium iodide (4). A solution of (**3**) (16.5 g, 52 mmol), methyl iodide (24.5 g, 0.17 mol), and benzene (200 mL) was stirred at RT for 48 h in darkness. The precipitated solid was filtered, washed with benzene (20 mL), and dried in vacuo to give a light-yellow solid (21.4 g, 89%); mp 164 °C (decomp). ^{1}H NMR (DMSO-d_6) δ: 2.89 (s, 9H), 3.84 (s, 3H), 5.21 (s, 2H), 7.08 (d, J = 8.6 Hz, 2H), 7.50 (m, 1H), 7.77 (m, 1H), 7.79 (d, 2H, J = 8.6 Hz), 9.24 (br s, 1H). ^{13}C NMR (DMSO-d_6) δ: 51.4, 55.2, 56.4, 109.8, 114.3, 118.0, 120.5, 123.3, 125.8, 127.3, 130.0, 144.2, 149.0, 159.5. MS ES(+ve) m/z 330 (M). Anal. ($C_{18}H_{21}ClIN_3O$) C, H, N.

2-(6-Chloro-2-(4-methoxyphenyl)imidazo[1,2-*a*]pyridin-3-yl)acetamide (5). A solution of (**4**) (21.4 g, 47 mmol), KCN (15.2 g, 0.23 mol), and ethanol/H_2O (1/1, 300 mL) was heated to reflux for 24 h. The solution was then cooled to RT and evaporated to dryness under a stream of nitrogen. Water (50 mL) was added and the solid filtered to collect a brown solid, which was dried in vacuo (13.9 g, 94%); mp 232−234 °C. ^{1}H NMR (DMSO-d_6) δ: 3.82 (s, 3H), 4.0 (s, 2H), 7.05 (d, J = 8.6 Hz, 2H), 7.24 (br s, 1H), 7.30 (dd, J = 9.5, 1.9 Hz, 1H), 7.53 (d, J = 9.5 Hz, 1H), 7.74 (d, 2H, J = 8.6 Hz), 7.80 (br s, 1H), 8.61 (d, J = 1.9 Hz, 1H). ^{13}C NMR (DMSO-d_6) δ: 32.1, 56.8, 115.7, 117.7, 118.9, 120.3, 124.5, 126.5, 128.2, 130.8, 143.8, 145.2, 160.6, 172.0. MS ES(+ve) m/z 316 (M + 1). Anal. ($C_{16}H_{14}ClN_3O_2$) C, H, N.

2-(6-Chloro-2-(4-hydroxyphenyl)imidazo[1,2-*a*]pyridin-3-yl)acetic acid hydrobromide hydrate (6). Compound (**5**) (13.7 g, 43 mol) was added to a solution containing 48% HBr (200 mL) and acetic acid (100 mL) and heated to 110 °C for 48 h. The solution was cooled to RT forming a light-brown precipitate. The solid was filtered, washed with acetic acid, and dried in vacuo (10.8 g, 63%); mp 260 °C (decomp). ^{1}H NMR (DMSO-d_6) δ: 4.26 (s, 2H), 7.03 (d, J = 8.0 Hz, 2H), 7.54 (d, J = 8.0 Hz, 2H), 7.94 (m, 2H), 9.28 (s, 1H), 10.15 (br s, 1H). ^{13}C NMR (DMSO-d_6) δ: 30.9, 114.9, 118.0, 118.3, 118.8, 125.1, 127.0, 131.6, 134.8, 136.8, 139.6 × 2, 161.1, 171.5. MS ES(+ve) m/z 303 (M + 1). Anal. ($C_{15}H_{11}ClN_2O_3 \cdot HBr.H_2O$) C, H, N.

2-(6-Chloro-2-(4-hydroxyphenyl)imidazo[1,2-*a*]pyridin-3-yl)-*N*,*N*-diethylacetamide (7). A mixture of (**6**) (1.15 g, 3.0 mmol), HOBT (405 mg, 3.0 mmol), DEA (372 μL, 3.6 mmol), and DIPEA (2.09 mL, 12.0 mmol) was dissolved with stirring in anhydrous DMF (8 mL). After 1 min, EDCI (748 mg, 3.90 mmol) was added and stirred for a further 18 h at RT. Water (60 mL) and acetic acid (0.5 mL) were then added, stirred for 1 min, and then placed at 4 °C for 6 h to give a precipitate which was filtered, washed with H_2O (20 mL), and dried in vacuo. Anhydrous DMF (3 mL) and DEA (0.5 mL) were then added to the crude product and heated to 100 °C for 2 h until the DEA was evaporated from the solution. After cooling to 80 °C, ethyl acetate (10 mL) was added rapidly and the mixture cooled to 5 °C for 4 h to form a white crystalline solid, which was washed with ethyl acetate (3 mL) and dried in vacuo (816 mg, 76%) as white needles; mp 226−228 °C. ^{1}H NMR (DMSO-d_6) δ: 1.06 (t, J = 7.1 Hz, 3H), 1.16 (t, J = 7.1 Hz, 3H), 3.32 (q, J = 7.1 Hz, 2H), 3.44 (q, J = 7.1 Hz, 2H), 4.18 (s, 2H), 6.83 (d, J = 8.8 Hz, 2H), 7.26 (dd, J = 9.4, 1.8 Hz, 1H), 7.41 (d, J = 8.8 Hz, 2H), 7.57 (d, J = 9.4 Hz, 1H), 8.49 (d, J = 1.8 Hz, 1H), 9.61 (br s, 1H). ^{13}C NMR (DMSO-d_6) δ: 13.0, 14.1, 28.7, 39.9, 41.6, 115.4, 116.1, 117.0, 118.3, 122.9, 124.5, 125.0, 129.1, 142.1, 143.9, 157.2, 167.1. MS ES(+ve) m/z 358 (M + 1). Anal. ($C_{19}H_{20}ClN_3O_2$) C, H, N.

2-(6-Chloro-2-(4-(2-fluoroethoxy)phenyl)imidazo[1,2-*a*]pyridin-3-yl)-*N*,*N*-diethylacetamide (8). A mixture of (**7**) (357 mg, 1.0 mmol), 1-bromo-2-fluoroethane (190 mg, 1.5 mmol), Bu_4NI (7.5 mg, 0.02 mmol), KI (25 mg, 0.15 mmol), and K_2CO_3 (207 mg, 1.5 mmol) in anhydrous DMF (2 mL) was stirred at 55 °C for 48 h before it was diluted with ethyl acetate (20 mL) and partitioned with water (10 mL). The organic layer was washed with water (3 × 5 mL), cold 2N NaOH (5 mL), water (3 × 5 mL), brine (5 mL), and then dried over Na_2SO_4. The dried organic solution was passed through a silica plug (1 × 0.5 cm) and elution continued with more ethyl acetate (10 mL). Evaporation of the solvent gave a yellow residue that was crystallized from ethyl acetate/hexane to give the title compound as pale-yellow flakes (287 mg, 71%); mp 140−142 °C. ^{1}H NMR (DMSO-d_6) δ: 1.06 (t, J = 7.0 Hz, 3H), 1.18 (t, J = 7.0 Hz, 3H), 3.34 (q, J = 7.0 Hz, 2H), 3.46 (q, J = 7.0 Hz, 2H), 4.22 (s, 2H), 4.30 (dm, J = 30.1 Hz, 2H), 4.78 (dm, J = 47.6 Hz, 2H), 7.08 (d, J = 9.1 Hz, 2H), 7.29 (dd, J = 9.4, 2.0 Hz, 1H), 7.55 (d, J = 9.1 Hz, 2H), 7.62 (d, J = 9.4 Hz, 1H), 8.52 (d, J = 2.0 Hz, 1H). ^{13}C NMR (DMSO-d_6) δ: 13.0, 14.1, 28.7, 39.9, 41.7, 67.1 (d, J = 18.8 Hz), 82.3 (d, J = 166.8 Hz), 114.7, 116.5, 117.1, 118.4, 123.0, 124.7, 127.0, 129.0, 142.2, 143.3, 157.9, 167.0. MS ES(+ve) m/z 404 (M + 1), 442 (M + K). Anal. ($C_{21}H_{23}ClFN_3O_2$) C, H, N.

2-(6-Chloro-2-(4-(2-hydroxyethoxy)phenyl)imidazo[1,2-*a*]pyridin-3-yl)-*N*,*N*-diethylacetamide (10a). A mixture of (**7**) (300 mg, 0.8 mmol), K_2CO_3 (442 mg, 3.2 mmol), KI (20 mg, 0.12 mmol), Bu_4NI (6 mg, 0.016 mmol), and anhydrous DMF (2 mL) was vigorously stirred for 2 min before 2-bromoethyl acetate (160 mg, 0.96 mmol) was added. The reaction was stirred at RT for 12 h, diluted with ethyl acetate (10 mL) and washed with water (3 × 10 mL), followed by brine (10 mL). The organic extract was dried (Na_2SO_4), filtered, and then concentrated in vacuo to give 2-(4-(6-chloro-3-(2-(diethylamino)-2-oxoethyl)imidazo[1,2-*a*]pyridin-2-yl)phenoxy)ethyl acetate (**9a**) as an orange solid (311 mg), which was hydrolyzed without further purification. ^{1}H NMR (DMSO-d_6) δ: 1.05 (t, J = 7.0 Hz, 3H), 1.16 (t, J = 7.0 Hz, 3H), 2.04 (s, 3H), 3.31 (q, J = 7.0 Hz, 2H), 3.44 (q, J = 7.0 Hz, 2H), 4.19 (s, 2H), 4.22 (m, 2H), 4.33 (m, 2H), 7.05 (d, J = 8.8 Hz, 2H), 7.28 (dd, J = 9.6, 2.0 Hz, 1H), 7.52 (d, J = 8.8 Hz, 2H), 7.60 (d, J = 9.6, 2.0 Hz, 1H), 8.50 (d, J = 2.0 Hz, 1H). The orange solid (**9a**) was dissolved in methanol (2 mL), and Cs_2CO_3 (443 mg, 1.36 mmol) in H_2O (1 mL) was added. After 48 h of stirring, at RT a precipitate had formed, which was collected by filtration and washed with water. The solid was recrystallized from ethyl acetate/hexane (1:1) to give the product as fine colorless needles (241 mg, 79%); mp 201−202 °C. ^{1}H NMR (DMSO-d_6) δ: 1.07 (t, J = 7.1 Hz, 3H), 1.17 (t, J = 7.1 Hz, 3H), 3.34 (q, J = 7.1 Hz, 2H), 3.45 (q, J = 7.1 Hz, 2H), 3.73 (dt, J = 5.3, 5.0 Hz, 2H), 4.03 (t, J = 5.0 Hz, 2H), 4.20 (s, 2H), 4.87 (t, J = 5.3 Hz, 1H), 7.03 (d, J = 8.8 Hz, 2H), 7.29 (dd, J = 9.5, 2.0 Hz, 1H), 7.52 (d, J = 8.8 Hz, 2H), 7.61 (dd, J = 9.5, 0.7 Hz, 1H), 8.50 (dd, J = 2.0, 0.7 Hz, 1H). ^{13}C NMR (DMSO-d_6) δ: 13.1, 14.1, 28.7, 39.9, 41.7, 59.6, 69.6, 114.6, 116.4, 117.1, 118.4, 123.0, 124.7, 126.5, 129.0, 142.2, 143.5, 158.4, 167.0. MS ES(+ve) m/z 402 (M + 1). Anal. ($C_{21}H_{24}ClN_3O_3$) C, H, N.

2-(6-Chloro-2-(4-(3-hydroxypropoxy)phenyl)imidazo[1,2-*a*]pyridin-3-yl)-*N*,*N*-diethylacetamide (10b). Compound (**7**) (268 mg, 0.75 mmol) was treated with 3-bromopropyl acetate (204 mg, 1.13 mmol), Bu_4NI (7 mg, 0.019 mmol), KI (19 mg, 0.11 mmol), and K_2CO_3 (206 mg, 1.5 mmol) in anhydrous DMF (1.5 mL) as described in the synthesis of (**10a**) to give 3-(4-(6-chloro-3-(2-(diethylamino)-2-oxoethyl)imidazo[1,2-*a*]pyridin-2-yl)phenoxy)propyl acetate (**9b**) as a pale-yellow solid (346 mg) that was used without further purification. ^{1}H NMR (DMSO-d_6) δ: 1.06 (t, J = 7.0 Hz, 3H), 1.17 (t, J = 7.0 Hz, 3H), 2.01 (s, 3H), 2.04 (m, 2H), 3.32 (q, J = 7.0 Hz, 2H), 3.44 (q, J = 7.0 Hz, 2H), 4.09 (t, J = 6.4 Hz, 2H), 4.17 (t, J = 6.4 Hz, 2H), 4.21 (s, 2H), 7.03 (d, J = 8.8 Hz, 2H), 7.28 (dd, J = 9.6, 2.0 Hz, 1H), 7.53 (d, J = 8.8 Hz, 2H), 7.60 (d, J = 9.6 Hz, 1H), 8.52 (d, J = 2.0 Hz, 1H). Compound (**9b**) was treated with Cs_2CO_3 (534 mg, 1.64 mmol) as described in the synthesis of (**10a**). Recrystallization of the resulting solid from ethanol/water gave colorless flakes of the title compound (277 mg, 89%); mp 119−120 °C. ^{1}H NMR (DMSO-d_6) δ: 1.07 (t, J = 7.0 Hz, 3H), 1.17 (t, J = 7.0 Hz, 3H), 1.88 (m, 2H), 3.33 (q, J = 7.0 Hz, 2H), 3.45 (q, J = 7.0 Hz, 2H), 3.59 (t, J = 6.0 Hz, 2H), 4.09 (t, J = 6.0 Hz, 2H), 4.22 (s, 2H), 4.58 (br s, 1H), 7.03 (d, J = 8.8 Hz, 2H), 7.29 (dd, J = 9.6, 2.0 Hz, 1H), 7.53 (d, J = 8.8 Hz, 2H), 7.61 (d, J = 9.6 Hz, 1H), 8.52 (d, J = 2.0 Hz, 1H). ^{13}C NMR (DMSO-d_6) δ: 13.0, 14.1, 28.6, 32.0, 39.7, 41.6, 57.2, 64.6, 114.4, 116.3, 117.0, 118.3, 122.9, 124.6, 126.4, 128.9, 142.1, 143.4, 158.3, 166.7. MS ES(+ve) m/z 416 (M + 1).

2-(4-(6-Chloro-3-(2-(diethylamino)-2-oxoethyl)imidazo[1,2-*a*]pyridin-2-yl)phenoxy)ethyl 4-methylbenzenesulfonate (11a). To a solution of (**10a**) (120 mg, 0.3 mmoL) in ethanol-free $CHCl_3$ (5 mL) at 40 °C was added TMHD (206 mg, 1.2 mmol), followed by *p*-toluenesulfonyl chloride (114 mg, 0.6 mmol). The solution was then cooled to RT and stirring continued for 15 h before it was washed with water (3 × 1 mL), aqueous tartaric acid (10%, 1 mL), and brine (5 mL). The organic solution was dried (Na_2SO_4), filtered, and concentrated in vacuo to give a light-yellow foam (102 mg, 60%). ^{1}H NMR (CD_3CN) δ: 1.15 (t, J = 7.0 Hz, 3H), 1.20 (t, J = 7.0 Hz, 3H), 2.46 (s, 3H), 3.43 (m, 4H), 4.13 (br s, 2H), 4.23 (m, 2H), 4.39 (m, 2H), 6.94 (d, J = 8.8 Hz, 2H), 7.26 (dd, J = 9.6, 1.8 Hz, 1H), 7.47 (d, J = 8.8 Hz, 2H), 7.55 (d, J = 9.6 Hz, 1H), 7.57 (d, J = 8.5 Hz, 2H), 7.84 (d, J = 8.5 Hz, 2H), 8.52 (d, J =

1.8 Hz, 1H). ^{13}C NMR (DMSO-d_6) δ: 13.0, 14.0, 21.0, 28.5, 39.8, 41.6, 65.3, 69.0, 114.6, 116.6, 116.7, 118.9, 123.2, 125.4, 126.1, 127.6, 128.9, 130.0, 132.2, 141.6, 142.2, 144.9, 157.5, 166.8. MS ES(+ve) *m/z* 556 (M + 1).

3-(4-(6-Chloro-3-(2-(diethylamino)-2-oxoethyl)imidazo[1,2-*a*]pyridin-2-yl)phenoxy)propyl 4-methylbenzenesulfonate (11b). . Compound (**10b**) (100 mg, 0.24 mmol) was treated with TMHD (86 mg, 0.5 mmol) and *p*-toluenesulfonyl chloride (92 mg, 0.48 mmol) as described for the synthesis of (**11a**). The resulting orange solid was recrystallized from ethyl acetate/hexane to give colorless needles (81 mg, 59%); mp 150−152 °C. ^{1}H NMR (CD_3CN) δ: 1.15 (t, J = 7.0 Hz, 3H), 1.23 (t, J = 7.0 Hz, 3H), 2.08 (m, 2H), 2.38 (s, 3H), 3.38 (q, J = 7.0 Hz, 2H), 3.42 (q, J = 7.0 Hz, 2H), 3.96 (t, J = 5.8 Hz, 2H), 4.10 (s, 2H), 4.22 (t, J = 5.8 Hz, 2H), 6.88 (d, J = 8.8 Hz, 2H), 7.25 (dd, J = 9.6, 1.8 Hz, 1H), 7.33 (d, J = 8.0 Hz, 2H), 7.53 (d, J = 8.8 Hz, 2H), 7.54 (d, J = 9.6 Hz, 1H), 7.75 (d, J = 8.0 Hz, 2H), 8.24 (d, J = 1.8 Hz, 1H). ^{13}C NMR (DMSO-d_6) δ: 13.0, 14.1, 21.0, 28.1, 28.6, 37.8, 41.6, 63.1, 67.5, 114.5, 116.4, 117.0, 118.6, 123.0, 125.4, 126.5, 127.5, 128.9, 130.1, 132.1, 142.3, 143.2, 144.8, 157.8, 167.0. MS ES(+ve) *m/z* 570 (M + 1).

2-(6-Chloro-2-(4-(3-fluoropropoxy)phenyl)imidazo[1,2-*a*]pyridin-3-yl)-*N,N*-diethylacetamide (12). To a stirred suspension of (**10b**) (62.3 mg, 0.15 mmol) in anhydrous acetonitrile (0.5 mL) was added DIPEA (158 μL, 0.9 mmol), PBSF (52 μL, 0.3 mmol), and TEA·3HF (50 μL, 0.3 mmol). The mixture was warmed to 50 °C to dissolve all the solids, and the solution was stirred at 40 °C for 2 h and RT for 12 h. Ethyl acetate (3 mL) was then added and the mixture washed with water (2 × 1 mL), brine (2 × 1 mL), dried over Na_2SO_4, and evaporated to give a glassy residue, which was purified by preparative HPLC on a Grace Alltima C18 column (10 μm, 22 mm × 250 mm), eluting with acetonitrile/H_2O + 0.1%TFA (40/60) at 10 mL/min. The major peak at 21.5 min was collected, evaporated to dryness, and redissolved in ethyl acetate (3 mL), washed with saturated $NaHCO_3$ solution, and dried (Na_2SO_4). The organic phase was concentrated in vacuo to give a white solid that was recrystallized from ethyl acetate/hexane to give the title compound as colorless needles (27.3 mg, 44%); mp 160−162 °C. ^{1}H NMR (CD_3CN) δ: 1.13 (t, J = 7.1 Hz, 3H), 1.18 (t, J = 7.1 Hz, 3H), 2.20 (m, 2H), 3.40 (q, J = 7.1 Hz, 2H), 3.44 (q, J = 7.1 Hz, 2H), 4.11 (s, 2H), 4.17 (t, J = 6.2 Hz, 2H), 4.67 (dt, J = 47.3, 5.9 Hz, 2H), 7.05 (d, J = 8.8 Hz, 2H), 7.24 (dd, J = 9.5, 2.0 Hz, 1H), 7.54 (dd, J = 9.5, 0.8 Hz, 1H), 7.58 (d, J = 8.8 Hz, 2H), 8.24 (dd, J = 2.0, 0.8 Hz, 1H). ^{13}C NMR (CD_3CN) δ: 13.3, 14.5, 30.2, 29.9 (d, J = 19.9 Hz), 41.1, 42.9, 64.7 (d, J = 5.4 Hz), 80.9 (d, J = 161.4 Hz), 115.6, 117.3, 118.1, 120.1, 123.6, 125.6, 128.0, 130.3, 143.8, 145.1, 159.6, 168.0. MS ES(+ve) *m/z* 418 (M + 1). Anal. ($C_{22}H_{25}ClFN_3O_2$) C, H, N.

***N,N*-Diethyl-2-(2-(4-hydroxyphenyl)-5,7-dimethylpyrazolo[1,5-*a*]pyrimidin-3-yl)acetamide (14).** *N,N*-Diethyl-2-(2-(4-methoxyphenyl)-5,7-dimethylpyrazolo[1,5-*a*]pyrimidin-3-yl)acetamide[48] (**13**) (730 mg, 2.0 mmol) and Bu_4NI (810 mg, 2.2 mmol) were dissolved in anhydrous dichloromethane (10 mL) under N_2. The mixture was cooled in an ethanol/liquid N_2 bath (−70 °C) and treated with BCl_3 in hexanes (9.0 mL, 9.0 mmol) over 5 min with vigorous stirring. After 5 min, the reaction was placed in an ice bath, and the mixture stirred for a further 2.5 h. Ice and water were added to quench the reaction and the mixture shaken vigorously with water (50 mL), chloroform (50 mL), and ethanol (5 mL). Solid $NaHCO_3$ was added in small portions to neutralize the acids from the hydrolysis of borate complexes. The organic layer was separated and the aqueous phase was further extracted with additional chloroform (2 × 20 mL). The combined organic extracts were washed with brine (50 mL), dried over Na_2SO_4, and evaporated to give a crystalline semisolid. This was slurried with acetonitrile (4 mL) and the colorless crystals collected by filtration (620 mg, 88%);mp 235−238 °C. ^{1}H NMR (DMSO-d_6) δ: 1.02 (t, J = 7.0 Hz, 3H), 1.17 (t, J = 7.0 Hz, 3H), 2.48 (s, 3H), 2.69 (s, 3H), 3.30 (q, J = 7.0 Hz, 2H), 3.51 (q, J = 7.0 Hz, 2H), 3.82 (s, 2H), 6.82 (s, 1H), 6.83 (d, J = 8.8 Hz, 2H), 7.58 (d, J = 8.8 Hz, 2H). ^{13}C NMR (DMSO-d_6) δ: 13.0, 14.1, 16.2, 24.1, 27.4, 40.4, 14.5, 100.3, 108.0, 115.1, 124.2, 129.2, 144.4, 147.1, 153.8, 157.1, 157.6, 169.0. MS ES(+ve) *m/z* 353 (M + 1). Anal. ($C_{20}H_{24}N_4O_2$) C, H, N.

2-(2-(4-(2-Fluoroethoxy)phenyl)-5,7-dimethylpyrazolo[1,5-*a*]pyrimidin-3-yl)-*N,N*-diethylacetamide (15). A mixture of (**14**) (176 mg, 0.5 mmol), 1-bromo-2-fluoroethane (49 μL, 0.65 mmol), Bu_4NI (3.7 mg, 0.01 mmol), K_2CO_3 (76 mg, 0.55 mmol), KI (12.5 mg 0.075 mmol), and anhydrous DMF (1 mL) was treated as described in the synthesis of (**8**). The product was recrystallized from ethyl acetate/hexane to give the title compound as a white solid (139 mg, 70%); mp 148−150 °C. ^{1}H NMR (DMSO-d_6) δ: 1.02 (t, J = 7.0 Hz, 3H), 1.18 (t, J = 7.0 Hz, 3H), 2.48 (s, 3H), 2.69 (s, 3H), 3.28 (q, J = 7.0 Hz, 1H), 3.52 (q, J = 7.0 Hz, 1H), 3.83 (s, 2H), 4.29 (dm J = 30.1 Hz, 2H), 4.76 (dm, J = 47.6 Hz, 2H), 6.84 (s, 1H), 7.06 (d, J = 8.8 Hz, 2H), 7.72 (d, J = 8.8 Hz, 2H). ^{13}C NMR (DMSO-d_6) δ: 13.1, 14.2, 16.3, 24.2, 27.5, 39.8, 41.6, 67.1 (d, J = 18.9 Hz), 82.1 (d, J = 166.0 Hz), 100.6, 108.3, 114.5, 126.3, 129.3, 144.5, 147.2, 153.4, 157.3, 158.3, 169.0. MS ES(+ve) *m/z* 399 (M + 1). Anal. ($C_{22}H_{27}FN_4O_2$) C, H, N.

***N,N*-Diethyl-2-(2-(4-(2-hydroxyethoxy)phenyl)-5,7-dimethylpyrazolo[1,5-*a*]pyrimidin-3-yl)acetamide (16a).** A mixture of (**14**) (264 mg, 0.75 mmol), 2-bromoethyl acetate (124 μL, 1.3 mmol), K_2CO_3 (310 mg, 2.25 mmol), KI (19 mg, 0.11 mmol), Bu_4NI (7 mg), and anhydrous DMF (1.5 mL) was treated as described for the synthesis of (**10a**). The resulting solid was recrystallized from ethanol/water to give white flakes of the title compound. (202 mg, 68%); mp 148−150 °C ^{1}H NMR (DMSO-d_6) δ: 1.02 (t, J = 7.0 Hz, 3H), 1.18 (t, J = 7.0 Hz, 3H), 2.49 (s, 3H), 2.70 (d, J = 0.8 Hz, 3H), 3.31 (q, J = 7.0 Hz, 2H), 3.52 (q, J = 7.0 Hz, 2H), 3.74 (dt, J = 5.5, 5.0 Hz, 2H), 3.84 (s, 2H), 4.04 (t, J = 5.0 Hz, 2H), 4.88 (t, J = 5.5 Hz, 1H), 6.84 (q, J = 0.8 Hz, 1H), 7.06 (d, J = 9.0 Hz, 2H), 7.72 (d, J = 9.0 Hz, 2H). ^{13}C NMR (DMSO-d_6) δ: 13.0, 14.1, 16.2, 24.1, 27.4, 39.8, 41.5, 59.5, 69.5, 100.3, 108.2, 114.3, 125.7, 129.1, 144.4, 147.1, 153.4, 157.2, 158.8, 168.9. MS ES(+ve) *m/z* 397 (M + 1). Anal. ($C_{22}H_{28}N_4O_3$) C, H, N.

***N,N*-Diethyl-2-(2-(4-(3-hydroxypropoxy)phenyl)-5,7-dimethylpyrazolo[1,5-*a*]pyrimidin-3-yl)acetamide (16b).** A mixture of (**14**) (352 mg, 1.0 mmol), 3-bromopropyl acetate (185 μL, 1.5 mmol), K_2CO_3 (414 mg, 3.0 mmol), KI (25 mg, 0.15 mmol), Bu_4NI (9 mg), and anhydrous DMF was treated as described for the synthesis of (**10a**). The resulting solid was recrystallized from ethanol/water to give pale-yellow needles of the title compound (282 mg, 69%); mp 116−118 °C. ^{1}H NMR (DMSO-d_6) δ: 1.02 (t, J = 7.0 Hz, 3H), 1.18 (t, J = 7.0 Hz, 3H), 1.88 (m, 2H), 2.49 (s, 3H), 2.70 (d, J = 0.9 Hz, 3H), 3.29 (q, J = 7.0 Hz, 2H), 3.52 (q, J = 7.0 Hz, 2H), 3.57 (td, J = 6.4, 5.3 Hz, 2H), 3.84 (s, 2H), 4.09 (t, J = 6.4 Hz, 2H), 4.56 (t, J = 5.3 Hz, 1H), 6.84 (q, J = 0.8 Hz, 1H), 7.02 (d, J = 8.8 Hz, 2H), 7.69 (d, J = 8.8 Hz, 2H). ^{13}C NMR (DMSO-d_6) δ: 13.0, 14.1, 16.2, 24.1, 27.4, 32.0, 39.7, 41.5, 57.2, 64.6, 100.4, 108.2, 114.3, 125.7, 129.2, 144.4, 147.1, 153.4, 157.2, 158.8, 169.0. MS ES(+ve) *m/z* 411 (M + 1). Anal. ($C_{23}H_{30}N_4O_3$) C, H, N.

2-(4-(3-(2-(Diethylamino)-2-oxoethyl)-5,7-dimethylpyrazolo[1,5-*a*]pyrimidin-2-yl)phenoxy)ethyl 4-methylbenzenesulfonate (17a). Compound (**16a**) (100 mg, 0.25 mmol) was treated with TMHD (150 μL, 0.7 mmol) and *p*-toluenesulfonyl chloride (96 mg, 0.5 mmol) in anhydrous acetonitrile (3 mL) as described in the synthesis of (**11a**). The resulting residue was evaporated in vacuo to give a light-brown foam of the title compound (120 mg, 88%). ^{1}H NMR (CD_3CN) δ: 1.11 (t, J = 7.0 Hz, 3H), 1.20 (t, J = 7.0 Hz, 3H), 2.45 (s, 3H), 2.54 (s, 3H), 2.75 (d, J = 0.9 Hz, 3H), 3.40 (q, J = 7.0 Hz, 2H), 3.51 (q, J = 7.0 Hz, 2H), 3.90 (s, 2H), 4.19 (m, 2H), 4.39 (m, 2H), 6.51 (q, J = 0.9 Hz, 1H), 6.86 (d, J = 8.8 Hz, 2H), 7.35 (d, J = 8.2 Hz, 2H), 7.75 (d, J = 8.8 Hz, 2H), 7.83 (d, J = 8.2 Hz, 2H). ^{13}C NMR (DMSO-d_6) δ: 13.0, 14.1, 16.1, 21.0, 24.1, 27.4, 40.1, 41.5, 65.3, 69.0, 100.5, 108.2, 114.3, 126.3, 127.6, 129.1, 130.0, 132.2, 144.4, 144.9, 147.1, 153.3, 157.2, 157.8, 168.9. MS ES(+ve) *m/z* 551 (M + 1). Anal. ($C_{29}H_{34}N_4O_5S$) C, H, N.

3-(4-(3-(2-(Diethylamino)-2-oxoethyl)-5,7-dimethylpyrazolo[1,5-*a*]pyrimidin-2-yl)phenoxy)propyl 4-methylbenzenesulfonate

(17b). Compound (**16b**) (100 mg, 0.24 mmol) was treated with TMHD (204 μL, 0.96 mmol) and *p*-toluenesulfonyl chloride (92 mg, 0.48 mmol) in anhydrous acetonitrile (5 mL) as described in the synthesis of (**11a**). The resulting solid was recrystallized from ethyl acetate to give the title compound as yellow crystals (114 mg, 84%); mp 141−143 °C. ^{1}H NMR ($CDCl_3$) δ: 1.11 (t, J = 7.0 Hz, 3H), 1.26 (t, J = 7.0 Hz, 3H), 2.12 (m, 2H), 2.39 (s, 3H), 2.49 (s, 3H), 2.74 (d, J = 0.9 Hz, 3H), 3.39 (q, J = 7.0 Hz, 2H), 3.57 (q, J = 7.0 Hz, 2H), 3.92 (s, 2H), 4.01 (t, J = 5.8 Hz, 2H), 4.26 (t, J = 6.1 Hz, 2H), 6.71 (q, J = 0.9 Hz, 1H), 6.90 (d, J = 8.8 Hz, 2H), 7.37 (d, J = 8.2 Hz, 2H), 7.74 (d, J = 8.8 Hz, 2H), 7.79 (d, J = 8.2 Hz, 2H). ^{13}C NMR (DMSO-d_6) δ: 13.0, 14.1, 16.2, 21.0, 24.1, 27.4, 28.0, 40.1, 41.5, 63.1, 67.5, 100.4, 108.2, 114.3, 126.0, 127.4, 129.1, 130.0, 132.1, 144.4, 144.8, 147.1, 153.4, 157.2, 158.2, 168.9. MS ES(+ve) m/z 565 (M + 1). Anal. ($C_{30}H_{36}N_4O_5S$) C, H, N.

***N*,*N*-Diethyl-2-(2-(4-(3-fluoropropoxy)phenyl)-5,7-dimethylpyrazolo[1,5-*a*]pyrimidin-3-yl)acetamide (18).** Compound (**16b**) (82 mg, 0.2 mmol) in anhydrous acetonitrile (0.8 mL) was treated with DIPEA (210 μL, 1.2 mmol), TEA.3HF (67 μL, 0.4 mmol), and PBSF (67 μL, 0.4 mmol) as described in the synthesis of (**12**). The resulting product was purified by preparative HPLC using a Grace Alltima C18 column (10 μm, 22 mm × 250 mm), eluting with acetonitrile/H_2O + 0.1%TFA (70/30), at 10 mL/min. The major peak at 15 min was collected and treated as described in the synthesis of (**12**) to give large white needles (48.6 mg, 59%); mp 106−108 °C. ^{1}H NMR (DMSO-d_6) δ: 1.02 (t, J = 7.1 Hz, 3H), 1.18 (t, J = 7.1 Hz, 3H), 2.14 (dm, J = 25.7 Hz, 2H), 2.49 (s, 3H), 2.69 (d, J = 0.8 Hz, 3H), 3.29 (q, J = 7.1 Hz, 2H), 3.52 (q, J = 7.1 Hz, 2H), 3.84 (s, 2H), 4.13 (t, J = 6.3 Hz, 2H), 4.58 (dm, J = 47.3 Hz, 2H), 6.84 (q, J = 0.8 Hz, 1H), 7.05 (d, J = 8.9 Hz, 2H), 7.70 (d, J = 8.9 Hz, 2H). ^{13}C NMR (DMSO-d_6) δ: 13.1, 14.2, 16.2, 24.2, 27.5, 29.7 (d, J = 19.6 Hz), 39.8, 41.6, 63.6 (d, J = 5.6 Hz), 80.8 (d, J = 161.6 Hz), 100.6, 108.3, 114.4, 126.1, 129.3, 144.6, 147.2, 153.5, 157.3, 158.6, 169.1. MS ES(+ve) m/z 413 (M + 1). Anal. ($C_{23}H_{29}FN_4O_2$) C, H, N.

Radiochemistry General Procedure. An aqueous [^{18}F]fluoride solution (6−7 GBq) was added to a 10 mL vial containing anhydrous acetonitrile (1 mL), $K_{2.2.2}$ and K_2CO_3. The solvent was evaporated under a stream of nitrogen at 100 °C under vacuum. This azeotropic drying was repeated twice by further addition of anhydrous acetonitrile (2 × 1 mL). The *p*-toluenesulfonyl precursor (**11a**), (**11b**), (**17a**), or (**17b**) (2 mg) was dissolved in anhydrous acetonitrile (1 mL) and added to the dried K[^{18}F]−$K_{2.2.2}$·K_2CO_3. complex. The reaction was stirred and heated at 100 °C for 5 min before the reaction mixture was diluted with mobile phase (500 μL) and purified by preparative reverse phase chromatography (Table 1). The collected radioactive peak was evaporated in vacuo and formulated to a concentration of 1 MBq/100 μL of saline containing less than 1% ethanol for biological studies.

Lipophilicity. The lipophilicity of **15**, **8**, **12**, and **18** was assessed using RP-HPLC by determining the log $P_{7.5}$ value using literature procedures.[51] Samples, dissolved in methanol, were analyzed using a Waters, Xterra C18 column (5 μm, 4.6 mm × 150 mm) with a mobile phase consisting of methanol/phosphate buffer (0.1 M, pH 7.5), 60/40 and a flow rate of 1 mL/min. The log $P_{7.5}$ of a studied compound was estimated by a comparison of its retention time to that of compounds of known log P value.

In Vitro Binding Assays. Kidney and brain cortical membranes were prepared as described previously.[52] The inhibition constant (IC_{50}) of the ligands for PBRs was determined by incubating, in triplicate, aliquots (0.3 mL) of diluted kidney membrane preparation (100−150 μg, protein) at 4 °C for 1 h with 7 concentrations of each studied compound (10^{-10} to 10^{-6} M) and [^{3}H]PK11195 (2 nM) or [^{3}H]Ro 5-4864 (1 nM) in a final volume of 0.5 mL. Nonspecific binding was determined with PK11195 (10 μM).

Similarly, the IC_{50} of the ligands for CBR was determined by incubating aliquots (0.3 mL), in triplicate, of diluted brain cortex membrane preparation (100−150 μg, protein) at 25 °C for 45 min with 7 concentrations of each studied compound (10^{-10} to 10^{-5} M) and of [^{3}H]flumazenil (2 nM) in a final volume of 0.5 mL. Nonspecific binding was determined with flumazenil (20 μM). In all cases, incubations were terminated by rapid filtration through Whatman GF/B glass fiber using a Brandel cell harvester. Filters were washed rapidly 3 times with 5 mL of ice-cold 50 mM Tris/HCl at pH 7.4. Filters were counted in a β-scintillation counter (Packard) to measure the amount of bound radioactivity. The IC_{50} of the compounds for the PBR and CBR were calculated using Kell 6 software. The IC_{50} values were converted to the inhibition constant, K_i, usingthe Cheng−Prussof equation and radioligand affinity values, [^{3}H]PK11195 (K_d = 2 nM), [^{3}H]Ro 5-4864 (K_d = 8 nM), and [^{3}H]flumazenil (K_d =1 nM).[6,53]

Biodistribution Studies. Animal experiments were performed in compliance with the NHMRC Australian Code of Practice for the care and use of animals for scientific purposes. [^{18}F]PBR radiotracers (1 MBq) were administered to 8−10 week old male SD rats via tail vein injection in a volume of 0.1 mL. At 0.25, 0.5, 1, and 4 h postinjection of the radiotracer, groups of rats (n = 4) were sacrificed by CO_2 administration followed by cervical fracture. Peripheral organs, (including liver, spleen, femur, thyroid, pancreas, lung, heart, kidney, and adrenals), blood, olfactory bulbs, and the remainder of the brain were removed. To investigate the uptake of radioactivity in the bone, bone marrow was also extracted from the medullar cavity of the femur and was analyzed in comparison to frontal skull bone. Samples of organs and tissues were weighed and the radioactivity was measured using an automated gamma counter. The percent injected dose (%ID) was calculated by comparison to a diluted standard solution derived from the initial injected solution. Radioactivity concentrations were expressed as percent of injected dose per gram of wet tissue (%ID/g).

Competition Studies. In saturation experiments, rats were injected intravenously with 1 mg/kg of unlabeled PBR compounds 5 min prior to injection of the respective [^{18}F]PBR compound (1 MBq). In competition experiments, the specificity of the [^{18}F]PBR was investigated by injecting in rats 5 min prior to the F-18 radioligands, 1 mg/kg flumazenil, Ro 5-4864, or PK11195 dissolved in dimethylsulfoxide/saline (1/1). The groups of rats (n = 4) were sacrificed at 1 h post injection and tissues were handled as described for the biodistribution studies. Radioactive concentrations in organs of treated animals were compared to the controls. Statistical significance was evaluated using one-way ANOVA. The criteria for significance were $p < 0.01$ and $p < 0.05$.

Metabolite Studies. The determination of unchanged radiotracer in the plasma, frontal cortex, and olfactory bulbs was performed by radio HPLC analysis, at 0.25, 0.5, 1, and 4 h after injection of 30 MBq of [^{18}F]PBR compounds. Plasma (100 μL) was mixed with 200 μL of water containing the PBR compound (10 nmol in 10 μL of CH_3OH) and KF (200 nmol) for direct injection onto the HPLC. Samples of brain tissue (100 mg) in 0.4 mL acetonitrile/water (1:1) containing unlabeled PBR compound and KF was exposed for 2 min to an ultrasonic probe and the mixture centrifuged at 3000 rpm for 10 min. The supernatant was collected and diluted with 1.5 mL of H_2O for HPLC analysis. The radioactivity of the precipitate was measured to quantify the acetonitrile/water extraction efficiency.

Radio-HPLC analysis was performed by adaptation of a literature procedure[54,55] using a precolumn (Waters Oasis HLB, 25 μm; 3.9 × 20 mm) and a reverse phase HPLC column (Waters X-terra, C18, 5 μm; 3.0 mm × 100 mm) in series, with a switching valve between columns. The precolumn was used to wash protein residue while trapping all nonpolar activity for subsequent gradient separation using the HPLC column. In the first step, the precolumn was washed with water for 5 min at 1 mL/min, and the fraction containing protein residue and nonlipophilic compounds bypassed the HPLC column by a switching valve and was sent through the UV and radioactivity detectors using a T-piece that was fitted post HPLC column. In the second step, the solvent direction was changed at 5 min to the HPLC column. Both columns in series were then eluted by gradient (10/90 to 90/10, CH_3CN/sodium acetate 0.05 M, pH 5.5) over 8 min at 1 mL/min. The radioactivity peak corresponding to the authentic PBR compound was compared to

the total activity registered in the radiochromatogram to give the fraction of unchanged ligand in the sample.

Acknowledgment. We gratefully acknowledge Donghai Jiang and Allira Schuster-Woodhouse for their support in the HPLC purification of the compounds and Tim Jackson for his QC support and log *P* measurements. We thank Thomas Bourdier for his excellent assistance in automated radiosynthesis and metabolite studies.

Supporting Information Available: Table of microanalytical data and HPLC purity test of target compounds **3**−**18.** This material is available free of charge via the Internet at http://pubs.acs.org.

References

(1) McEnery, M. W.; Snowman, A. M.; Trifiletti, R. R.; Snyder, S. H. Isolation of the mitochondrial benzodiazepine receptor: association with the voltage-dependent anion channel and the adenine nucleotide carrier. *Proc. Natl. Acad. Sci. U.S.A.* **1992**, *89*, 3170–3174.

(2) Anholt, R. R.; De Souza, E. B.; Oster-Granite, M. L.; Snyder, S. H. Peripheral-type benzodiazepine receptors: autoradiographic localization in whole-body sections of neonatal rats. *J. Pharmacol. Exp. Ther.* **1985**, *233*, 517–526.

(3) Benavides, J.; Quarteronet, D.; Imbault, F.; Malgouris, C.; Uzan, A.; Renault, C.; Dubroeucq, M. C.; Gueremy, C.; Le Fur, G. Labelling of "peripheral-type" benzodiazepine binding sites in the rat brain by using PK 11195, an isoquinoline carboxamide derivative: kinetic studies and autoradiographic localization. *J. Neurochem.* **1983**, *41*, 1744–1750.

(4) Papadopoulos, V.; Amri, H.; Boujrad, N.; Cascio, C.; Culty, M.; Garnier, M.; Hardwick, M.; Li, H.; Vidic, B.; Brown, A. S.; Reversa, J. L.; Bernassau, J. M.; Drieu, K. Peripheral benzodiazepine receptor in cholesterol transport and steroidogenesis. *Steroids* **1997**, *62*, 21–28.

(5) Schoemaker, H.; Bliss, M.; Yamamura, H. I. Specific high-affinity saturable binding of Ro 5-4864 to benzodiazepine binding sites in the rat cerebral cortex. *Eur. J. Pharmacol.* **1981**, *71*, 173–175.

(6) Awad, M.; Gavish, M. Binding of [3H]Ro 5-4864 and [3H]PK 11195 to cerebral cortex and peripheral tissues of various species: species differences and heterogeneity in peripheral benzodiazepine binding sites. *J. Neurochem.* **1987**, *49*, 1407–1414.

(7) Benavides, J.; Fage, D.; Carter, C.; Scatton, B. Peripheral type benzodiazepine binding sites are a sensitive indirect index of neuronal damage. *Brain. Res.* **1987**, *421*, 167–172.

(8) Vowinckel, E.; Reutens, D.; Becher, B.; Verge, G.; Evans, A.; Owens, T.; Antel, J. P. PK11195 binding the peripheral benzodiazepine receptor as a marker or microglia activation in multiple sclerosis and experimental autoimmune encephalomyelitis. *J. Neurosci. Res.* **1997**, *50*, 345–353.

(9) Diorio, D.; Welner, S. A.; Butterworth, R. F.; Meaney, M. J.; Suranyl-Cadotte, B. E. Peripheral benzodiazepine binding sites in Alzheimer's disease frontal cortex and temporal cortex. *Neurobiol. Aging* **1991**, *12*, 255–258.

(10) McGeer, E. G.; Singh, E. A.; McGeer, P. L. Peripheral-type benzodiazepine binding in Alzheimer disease. *Alzheimer Dis. Assoc. Disord.* **1988**, *2*, 331–336.

(11) McGeer, P. L.; Itagaki, S.; Boyes, B. E.; McGeer, E. G. Reactive microglia are positive for HLA-DR in the substantia nigra of Parkinson's and Alzheimer's disease brains. *Neurology* **1988**, *38*, 1285–1291.

(12) Ouchi, Y. Y. E. Microglial activation and dopamine terminal loss in early Parkinson's disease. *Ann. Neurol.* **2005**, *57*, 168–175.

(13) Messmer, K.; Reynolds, G. P. Increased peripheral benzodiazepine binding sites in the brain of patients with Huntingtons disease. *Neurosci. Lett.* **1998**, *241*, 53–56.

(14) Banati, R. B.; Newcombe, J.; Gunn, R. N.; Cagnin, A.; Turkheimer, F.; Heppner, F.; Price, G.; Wegner, F.; Giovannoni, G.; Miller, D. H.; Perkin, G. D.; Smith, T.; Hewson, A. K.; Bydder, G.; Kreutzberg, G. W.; Jones, T.; Cuzner, M. L.; Myers, R. The peripheral benzodiazepine binding site in the brain in multiple sclerosis: Quantitative in vivo imaging of microglia as a measure of disease activity. *Brain* **2000**, *123*, 2321–2337.

(15) Black, K. L.; Ikezaki, K.; Santori, E.; Becker, D. P.; Vinters, H. V. Specific high-affinity binding of peripheral benzodiazepine receptor ligands to brain tumors in rat and man. *Cancer* **1990**, *65*, 93–97.

(16) Junck, L.; Olson, J. M.; Ciliax, B. J.; Koeppe, R. A.; Watkins, G. L.; Jewett, D. M.; McKeever, P. E.; Wieland, D. M.; Kilbourn, M. R.; Starosta-Rubinstein, S. PET imaging of human gliomas with ligands for the peripheral benzodiazepine binding site. *Ann. Neurol.* **1989**, *26*, 752–758.

(17) Hardwick, M.; Fertikh, D.; Culty, M.; Li, H.; Vidic, B.; Papadopoulos, V. Peripheral-type benzodiazepine receptor (PBR) in human breast cancer: correlation of breast cancer cell aggressive phenotype with PBR expression, nuclear localization, and PBR-mediated cell proliferation and nuclear transport of cholesterol. *Cancer Res.* **1999**, *59*, 831–842.

(18) Katz, Y.; Eitan, A.; Amiri, Z.; Gavish, M. Dramatic increase in peripheral benzodiazepine binding sites in human colonic adenocarcinoma as compared to normal colon. *Eur. J. Pharmacol.* **1988**, *148*, 483–484.

(19) Katz, Y.; Ben-Baruch, G.; Kloog, Y.; Menczer, J.; Gavish, M. Increased density of peripheral benzodiazepine-binding sites in ovarian carcinomas as compared with benign ovarian tumours and normal ovaries. *Clin. Sci. (London)* **1990**, *78*, 155–158.

(20) Batra, S.; Alenfall, J. Characterization of peripheral benzodiazepine receptors in rat prostatic adenocarcinoma. *Prostate (N.Y.)* **1994**, *24*, 269–278.

(21) Pike, V. W.; Halldin, C.; Crouzel, C.; Barre, L.; Nutt, D. J.; Osman, S.; Shah, F.; Turton, D. R.; Waters, S. L. Radioligands for PET studies of central benzodiazepine receptors and PK (peripheral benzodiazepine) binding sites-current status. *Nucl. Med. Biol.* **1993**, *20*, 503–525.

(22) Gildersleeve, D. L.; Lin, T. Y.; Wieland, D. M.; Ciliax, B. J.; Olson, J. M.; Young, A. B. Synthesis of a high specific activity 125I-labeled analog of PK11195, potential agent for SPECT imaging of the peripheral benzodiazepine binding site. *Int. J. Rad. Appl. Instrum. B* **1989**, *16*, 423–429.

(23) Gildersleeve, D. L.; Van Dort, M. E.; Johnson, J. W.; Sherman, P. S.; Wieland, D. M. Synthesis and evaluation of ^{123}I-iodo-PK11195 for mapping peripheral-type benzodiazepine receptors (omega 3) in heart. *Nucl. Med. Biol.* **1996**, *23*, 23–28.

(24) Katsifis, A.; Mattner, F.; Mardon, K.; Papazian, V.; Dikic, B. Imidazo[1,2-*a*]pyridines as peripheral benzodiazepine receptor binding agents. WO Patent, 9951594, 1999.

(25) Katsifis, A.; Mattner, F.; Dikic, B.; Papazian, V. Synthesis of substituted [123I]imidazo[1,2-*a*]pyridines as potential probes for the study of the peripheral benzodiazepine receptors using SPECT. *Radiochim. Acta* **2000**, *88*, 229–232.

(26) Katsifis, A.; Mattner, F.; Mardon, K.; Papazian, V.; Dikic, B. Evaluation of [^{123}I]Imidazo[1,2-*a*]pyridines as potential probes for the study of the peripheral benzodiazepine receptors using SPECT. *J. Nucl. Med.* **1998**, *5*, P50.

(27) Thominiaux, C.; Mattner, F.; Greguric, I.; Boutin, H.; Chauveau, F.; Kuhnast, B.; Gregoire, M. C.; Loc'h, C.; Valette, H.; Bottlaender, M.; Hantraye, P.; Tavitian, B.; Katsifis, A.; Dolle, F. Radiosynthesis of 2-[6-chloro-2-(4-iodophenyl)Imidazo [1,2-*a*]pyridin-3-yl]-*N*-ethyl-*N*-[C-11]methyl-acetamide, [C-11]CLINME, a novel radioligand for imaging the peripheral benzodiazepine receptors with PET. *J. Labelled. Compd. Radiopharm.* **2007**, *50*, 229–236.

(28) Mattner, F.; Pham, T.; Greguric, I.; Berghoffer, P.; Ballantyne, P.; Liu, X.; Dikic, D.; Jackson, T.; Dolle, F.; Katsifis, A. Labelling and in vivo evaluation of the [^{123}I] labelled Imidazopyridine-3-acetamide, CLINME for the study of the peripheral benzodiazepine binding sites. *J. Labelled. Compd. Radiopharm.* **2007**, *50*, S31.

(29) Katsifis, A.; Fookes, C. J. R.; Pham, T. Q.; Greguric. I.; Mattner, F. Fluorinated ligands for targeting peripheral benzodiazepine receptors. AUS Patent 2006904617, 2007.

(30) James, M. L.; Fulton, R. R.; Henderson, D. J.; Eberl, S.; Meikle, S. R.; Thomson, S.; Allan, R. D.; Dolle, F.; Fulham, M. J.; Kassiou, M. Synthesis and in vivo evaluation of a novel peripheral benzodiazepine receptor pet radioligand. *Bioorg. Med. Chem.* **2005**, *13*, 6188–6194.

(31) Homes, T. P.; Mattner, F.; Keller, P. A.; Katsifis, A. Synthesis and in vitro binding of *N,N*-dialkyl-2-phenylindol-3-yl-glyoxylamides for the peripheral benzodiazepine binding sites. *Bioorg. Med. Chem.* **2006**, *14*, 3938–3946.

(32) Maeda, J.; Suhara, T.; Zhang, M. R.; Okauchi, T.; Yasuno, F.; Ikoma, Y.; Inaji, M.; Nagai, Y.; Takano, A.; Obayashi, S.; Suzuki, K. Novel peripheral benzodiazepine receptor ligand [C-11]DAA1106 for PET: an imaging tool for glial cells in the brain. *Synapse* **2004**, *52*, 283–291.

(33) Zhang, M. R.; Ogawa, M.; Maeda, J.; Ito, T.; Noguchi, J.; Kumata, K.; Okauchi, T.; Suhara, T.; Suzuki, K. [2-C-11]isopropyl-, [1-C-11]ethyl-, and [C-11]methyl-labeled phenoxyphenyl acetamide derivatives as positron emission tomography ligands for the peripheral benzodiazepine receptor: radiosynthesis, uptake, and in vivo binding in brain. *J. Med. Chem.* **2006**, *49*, 2735–2742.

(34) Briard, E.; Zoghbi, S. S.; Imaizumi, M.; Gourley, J. P.; Shetty, H. U.; Hong, J.; Cropley, V.; Fujita, M.; Innis, R. B.; Pike, V. W. Synthesis and evaluation in monkey of two sensitive ^{11}C-labeled aryoxyanilide ligands imaging brain peripheral benzodiazepine receptors in vivo. *J. Med. Chem.* **2008**, *51*, 17–30.

(35) Zhang, M. R.; Maeda, J.; Ogawa, M.; Noguchi, J.; Ito, T.; Yoshida, Y.; Okauchi, T.; Obayashi, S.; Suhara, T.; Suzuki, K. Development

of a new radioligand, *N*-(5-fluoro-2-phenoxyphenyl)-*N*-(2-[^{18}F]fluoroethoxy-5-methoxybenzyl)acetamide, for PET imaging of peripheral benzodiazepine receptor in primate brain. *J. Med. Chem.* **2004**, *47*, 2228–2235.

(36) Imaizumi, M.; Briard, E.; Zoghbi, S. S.; Gourley, J. P.; Hong, J.; Musachio, J. L.; Gladding, R.; Pike, V. W.; Innis, R. B.; Fujita, M. Kinetic evaluation in nonhuman primates of two new PET ligands for peripheral benzodiazepine receptors in brain. *Synapse* **2007**, *61*, 595–605.

(37) Pham, T.; Fookes, C.; Liu, X.; Greguric, I.; Bourdier, T.; Katsifis, A. Synthesis of [^{18}F]Fluorine labelled imidazo[1,2*b*]pyridazine as potential probes for the study of peripheral benzodiazepine binding sites using PET. *J. Labelled. Compd. Radiopharm.* **2007**, *50*, S204.

(38) Trapani, G.; Franco, M.; Ricciardi, L.; Latrofa, A.; Genchi, G.; Sanna, E.; Tuveri, F.; Cagetti, E.; Biggio, G.; Liso, G. Synthesis and binding affinity of 2-phenylimidazo[1,2-*a*]pyridine derivatives for both central and peripheral benzodiazepine receptors. A new series of high-affinity and selective ligands for the peripheral type. *J. Med. Chem.* **1997**, *40*, 3109–3118.

(39) Selleri, S.; Bruni, F.; Costagli, C.; Costanzo, A.; Guerrini, G.; Ciciani, G.; Aiello, P. M.; Lamberti, C.; Costa, B.; Martini, C. Synthesis and BZR affinity of pyrazolo[1,5-*a*]pyrimidine derivatives. Part 2: Further investigations on the 3-aryl substituents. *Med. Chem. Res.* **2000**, *10*, 92–113.

(40) Kaestle, K. L.; Anwer, M. K.; Audhya, T. K.; Goldstein, G. Cleavage of esters using carbonates and bicarbonates of alkali metals: synthesis of thymopentin. *Tetrahedron Lett.* **1991**, *32*, 327–330.

(41) Yin, J.; Zarkowsky, D. S.; Thomas, D. W.; Zhao, M. M.; Huffman, M. A. Direct and convenient conversion of alcohols to fluorides. *Org. Lett.* **2004**, *6*, 1465–1468.

(42) Brooks, P. R.; Wirtz, M. C.; Vetelino, M. G.; Rescek, D. M.; Woodworth, G. F.; Morgan, B. P.; Coe, J. W. Boron trichoride/tetra-*n*-butylammonium iodide: a mild, selective combination reagent for the cleavage of primary alkyl aryl ethers. *J. Org. Chem.* **1999**, *64*, 9719–9721.

(43) McMahon, R. E. Microsomal dealkylation of drugs, substrate specificity and mechanism. *J. Pharm. Sci.* **1966**, *55*, 457–466.

(44) Axelrod, J. The enzymatic cleavage of aromatic ethers. *J. Biochem.* **1956**, *63*, 634–639.

(45) Zoghbi, S. S.; Shetty, H. U.; Ichise, M.; Fujita, M.; Imaizumi, M.; Liow, J.-S.; Shah, J.; Musachio, J. L.; Pike, V. W.; Innis, R. B. PET imaging of the dopamine transporter with ^{18}F-FECNT: a polar radiometabolite confounds brain radioligand measurements. *J. Nucl. Med.* **2006**, *47*, 520–527.

(46) Knust, E. J.; Kupfernagel, C.; Stöcklin, G. Long-chain F-18 fatty acids for the study of regional metabolism in heart and liver; odd-even effects of metabolism in mice. *J. Nucl. Med.* **1979**, *20*, 1170–1175.

(47) Langer, S. Z.; Arbilla, S.; Benavides, J.; Scatton, B. Zolpidem and alpidem: two imidazopyridines with selectivity for ω1- and ω3-receptor subtypes. *Adv. Biochem. Psychopharmacol.* **1990**, *46*, 61–72.

(48) Pisu, M. G.; Papi, G.; Porcu, P.; Trapani, G.; Latrofa, A.; Biggio, G.; Serra, M. Binding of [3H]CB 34, a selective ligand for peripheral benzodiazepine receptors, to rat brain membranes. *Eur. J. Pharmacol.* **2001**, *432*, 129–134.

(49) Selleri, S.; Bruni, F.; Costagli, C.; Costanzo, A.; Guerrini, G.; Ciciani, G.; Costa, B.; Martini, C. 2-arylpyrazolo[1,5-*a*]pyrimidin-3-yl acetamides. New potent and selective peripheral benzodiazepine receptor ligands. *Bioorg. Med. Chem.* **2001**, *9*, 2661–2671.

(50) Oae, S. Relative reactivities of organic halides in displacement reactions. Reactions of mercuric nitrate with some bromoketones, bromoesters and bromoethers. *J. Am. Chem. Soc.* **1956**, *78*, 4030–4032.

(51) Waterhouse, R. N. Determination of lipophilicity and its use as a predictor of blood brain barrier penetration of molecular imaging agents. *Mol. Imaging Biol.* **2003**, *5*, 376–389.

(52) Mattner, F.; Mardon, K.; Loc'h, C.; Katsifis, A. Pharmacological evaluation of a labelled imidazopyridine-3-acetamide for the study of benzodiazepine receptors. *Life Sci.* **2006**, *79*, 287–294.

(53) Fonia, O.; Weizman, R.; Zisman, E.; Ashkenazi, R.; Gavish, M. Down-regulation of hepatic peripheral-type benzodiazepine receptors caused by acute lead intoxication. *Eur. J. Pharmacol.* **1995**, *293*, 335–339.

(54) Hilton, J.; Yokoi, F.; Dannals, R. F.; Hayden, H. T.; Szabo, Z.; Wong, D. F. Column-switching HPLC for the analysis of plasma in PET imaging studies. *Nucl. Med. Biol.* **2000**, *27*, 627–630.

(55) Wilson, A. A.; McCormick, P.; Kapur, S.; Willeit, M.; Garcia, A.; Hussey, D.; Houle, S.; Seeman, P.; Ginovart, N. Radiosynthesis and evaluation of [^{11}C]-4-propyl-3,4,4*a*,5,6,10*b*-hexahydro-2*H*-naphtho[1,2-*b*][1,4]oxazin-9-ol as a potential radiotracer for in vivo imaging of the dopamine D2 high-affinity state with positron emission tomography. *J. Med. Chem.* **2005**, *48*, 4153–4160.

JM7014556